Quarterly Report

Project Title:
Development of a Self-Sustained Wireless Integrated Structural
Health Monitoring System for Highway Bridges

Cooperative Agreement # RITARS11HUMD

Tenth Quarterly Progress Report

Period:
October 15, 2013 through January 14, 2014

Submitted by:
The Research Team – University of Maryland with North
Carolina State University and URS

Submitted to:
Mr. Caesar Singh, Program Manager, US DOT

Date: February 12, 2014

Table of Contents

Attachment (Status report to MD SHA)

    Field Test Status Report of MD Bridge No. 1504200 I-270 over Middlebrook Road

I — TECHNICAL STATUS

Accomplishments by Milestone

1.1.   General
- Updated Project web site (http://www.ncrst.umd.edu/) (Task 1 and Deliverable 2)
- Delivered ninth quarterly financial and technical reports (Task 6 and Deliverable 11)
- Conducted group meeting with URS dated Jan. 22, 2014 on the summary of the past pilot bridge, I-270 over Middlebrook Road, and checked the status of the future demo bridge, I-95 over Patuxent River, and other possibilities.
- Attended TRB conference & NDE committee meeting in January 2014 in Washington, DC
- Plan to attend ASNT conference in August 2014 and delivered two abstracts.
- The revised work plan is shown below as Milestones/Deliverables. Dark Shading indicates Deliverable items and Tasks in which the Research Team has been engaged over the past quarters. Lighter shading indicates anticipated duration for Deliverables by quarters. Grid pattern shading means partially fulfilled.

Deliverables	Action	Quarter No.											
		1	2	3	4	5	6	7	8	9	10	11	12
1	Form TAC and conduct kick-off meeting. Determine baseline field test procedure (Task 1)	■											
2	Establish and update project web site (Tasks 1 & 6)	■	■	■	■	■	■	■	■	■	■	▨	▨
3	Conduct baseline field test and finite element analysis on pre-selected bridges (Task 1)	■	■										
4	Design, fabricate and characterize AE sensor and measure the performance (Task 2)	■	■	■									
5	Develop and evaluate T-R method for passive damage interrogation (Task 3)	■	■	■	■								
6	Develop and experimentally evaluate wireless smart sensor and hybrid-mode energy harvester (Task 4)	■	■	■	■	■							
7	Implement passive damage interrogation T-R algorithm in the wireless smart sensor on bridges (Task 4)	■	■	■	■	■	■	■	■	■	▨		
8	Integrate and validate AE sensors with wireless smart sensor and hybrid-mode energy harvester (Task 5)	■	■	■	■	■	■	■	■	■	▨	▨	▨
9	Develop and conduct field implementation/validation of commercial-ready ISHM system with remote sensing capability (Task 5)	■	■	■	■	■	■	■	■	■	▨	▨	▨
10	Recommend strategy to incorporate remote sensing and prognosis into BMS (Task 5)	■	■	■	■	■	■	■	■	■	▨	▨	▨
11	Prepare and submit quarterly status and progress reports and final project report (Task 6)	■	■	■	■	■	■	■	■	■	■	▨	▨
12	Submit paper to conference presentations and publication to TRB meeting or other conferences (Task 6)	■	■	■	■	■	■	■	■	■	■	▨	▨

Note: Deliverables items 7, 8, 9 and 10 for the 8th quarter are partially fulfilled. They are still tested and modified by the NCSU team. The explanation of the delay is described and highlighted later under Section 1.6 - Future Plan.

1.2.   Remote Health Monitoring System
- Continued extrapolation analysis of acquired stress data
- Reconfigured hardware to address malfunctions with strain sensors
- Explored differences between linear and nonlinear accumulation models
- Researched approaches for obtaining and estimating Stress Intensity Factors
- Configured Microstrian™ Wireless Sensor Network

- Installed software and hardware of Microstrain™ onto National Instruments Data Acquisition System (PXI)
- Configured and calibrated new Microstrain™ equipment to work with BDI strain gauge sensors.
- Working on I270 bridge dynamic performance under truck loading using ANSYS APDL
  - 3D finite element bridge model subjected to a moving vehicle
  - 3D finite element bridge model bridge subjected to a dynamic vehicle system (moving mass with spring and damper)
  - Vehicle-bridge interaction considering road roughness

- Working on the influence on the stress of connection plates with or without top chords
  - The maximum axial force of top chords is small, around 2-3 kips, while the maximum axial forces of other chords are around 5 kips.
  - The stress of some elements of connection plates changes a lot. The conclusion can be reached after more elements have been checked.

1.3   Pilot Bridge Test and following activities
- Summary of MD Bridge No. 1504200 I-270 over Middlebrook Road, (also submitted to the MDSHA) is in the Attachment of this report.

1.4   AE Sensor
- To enhance the sensitivity of piezoelectric film sensor, a 54-dB gain preamplifier has been design and a prototype amplifier board was fabricated and tested in UMD lab. This amplifier was verified to achieve a 54-dB gain in amplifying the signal from piezo paint AE sensor.
- Test of the piezo film acoustic emission sensor was carried out on full scale steel plate fracture tests: The test specimen is a full scale steel plate wall under low cycle fatigue loading. At the end of its low-cycle fatigue life, the steel plate fractured at the slot corner location. Acoustic emission monitoring of steel plate low cycle fatigue induced crack with piezo film acoustic emission sensor was performed on steel plate wall and results are shown in Figure 1. Fatigue crack growth monitoring with piezo film AE sensor was terminated on I-270 bridge on September 27, 2013 and all field test equipment were removed from the bridge.
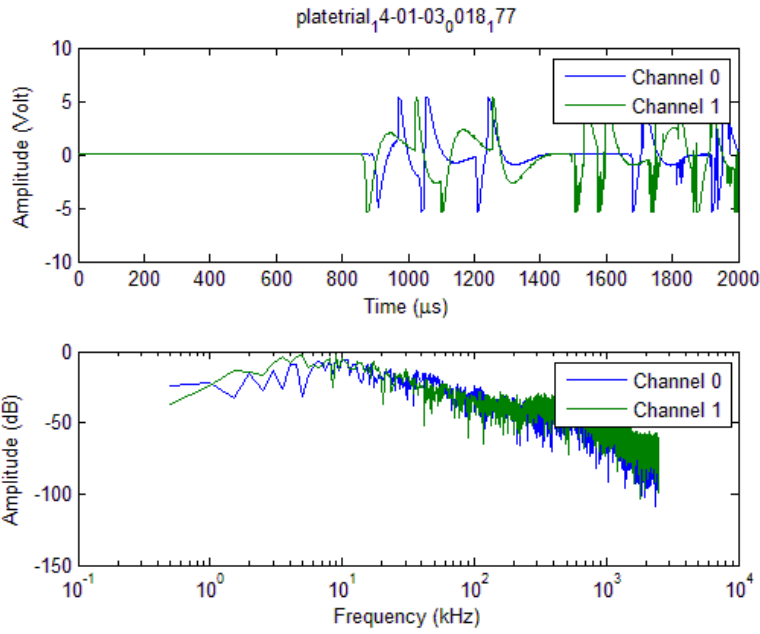
Figure 1. Acoustic emission signal recorded by the piezo film AE sensors when the steel plate fractured
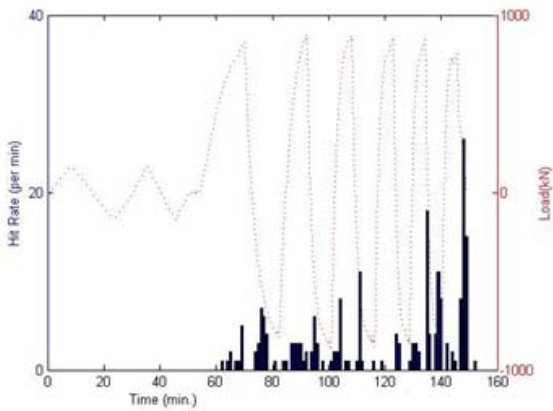

Figure 2. Variation of AE hit rates and cyclic fatigue loading with time

1.5   T-R Method, Energy Harvesting and Smart Sensor

Accomplishments of these tasks by NCSU team are summarized here:
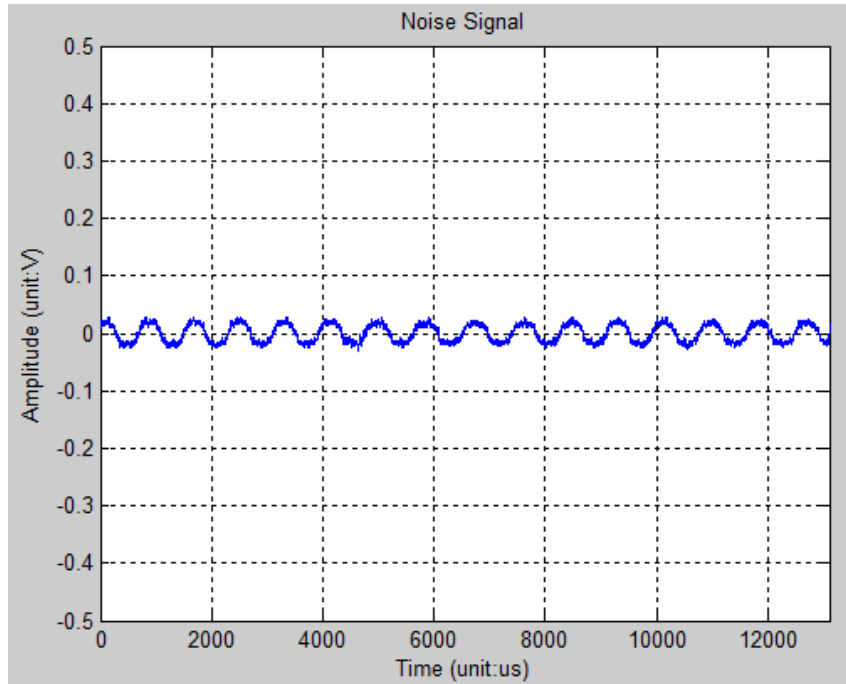1.   Test the noise signal of the piezoelectric sensor in the lab.
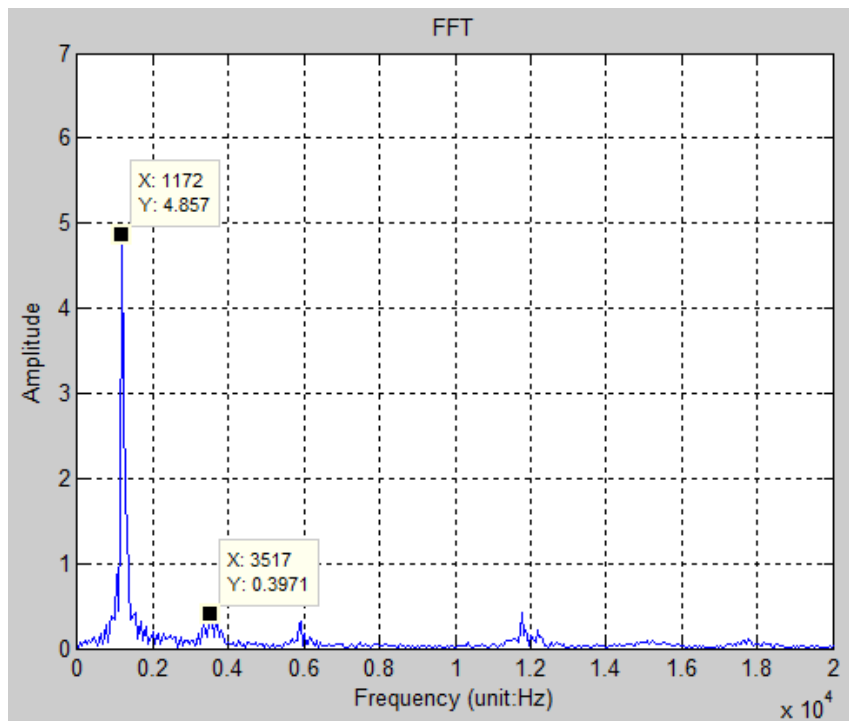
Figure 3a. Noise signal waveform (Set 1)
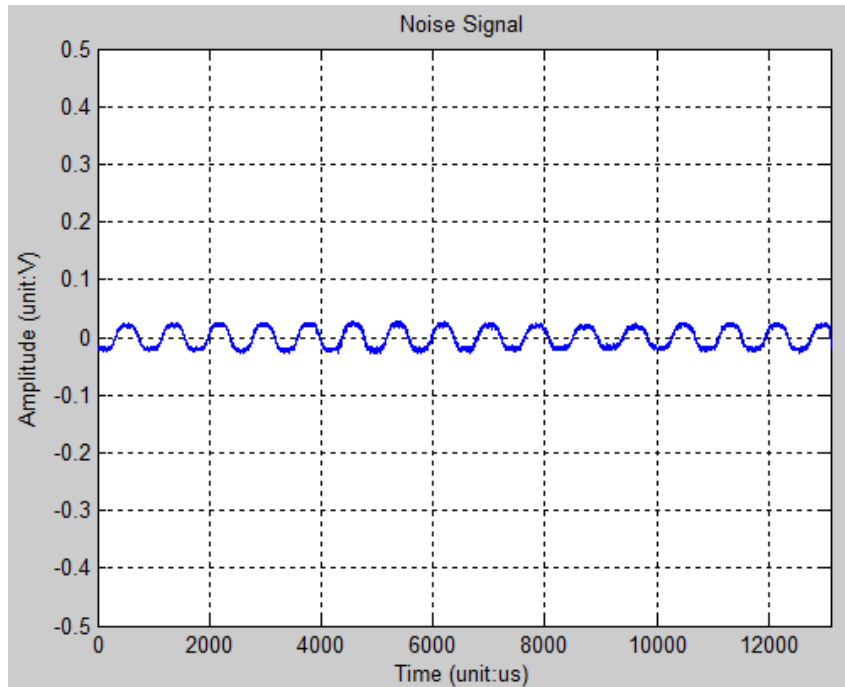
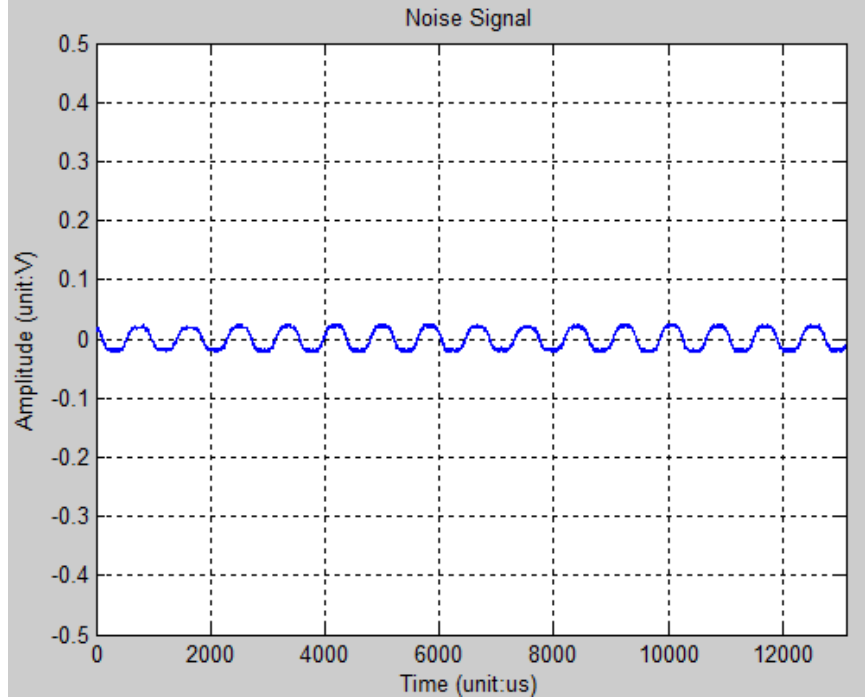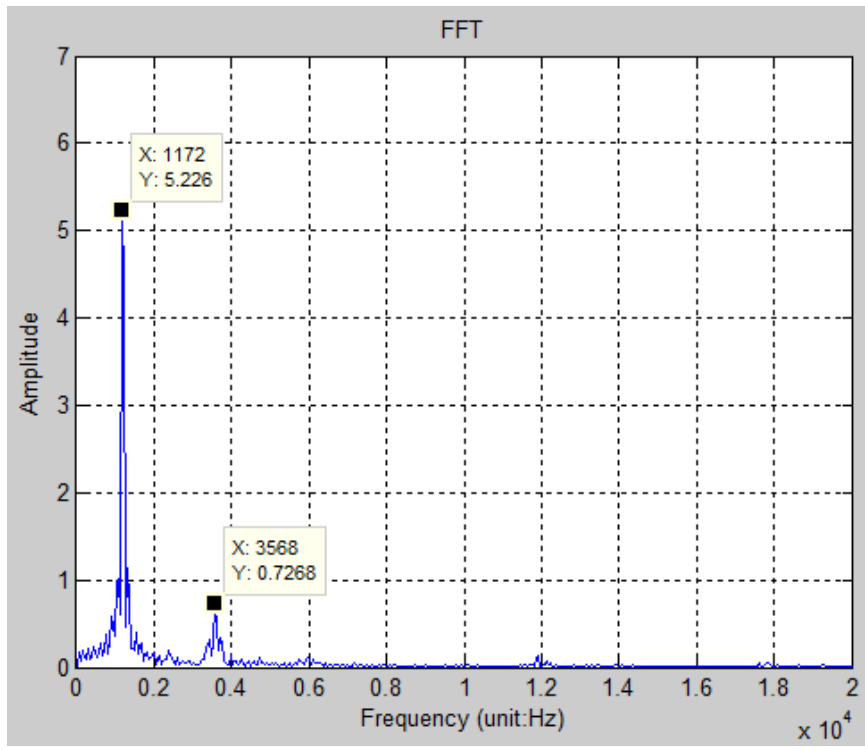Figure 3b. FFT of noise signal (Set 1)

Figure 4a. Noise signal waveform (Set 2)
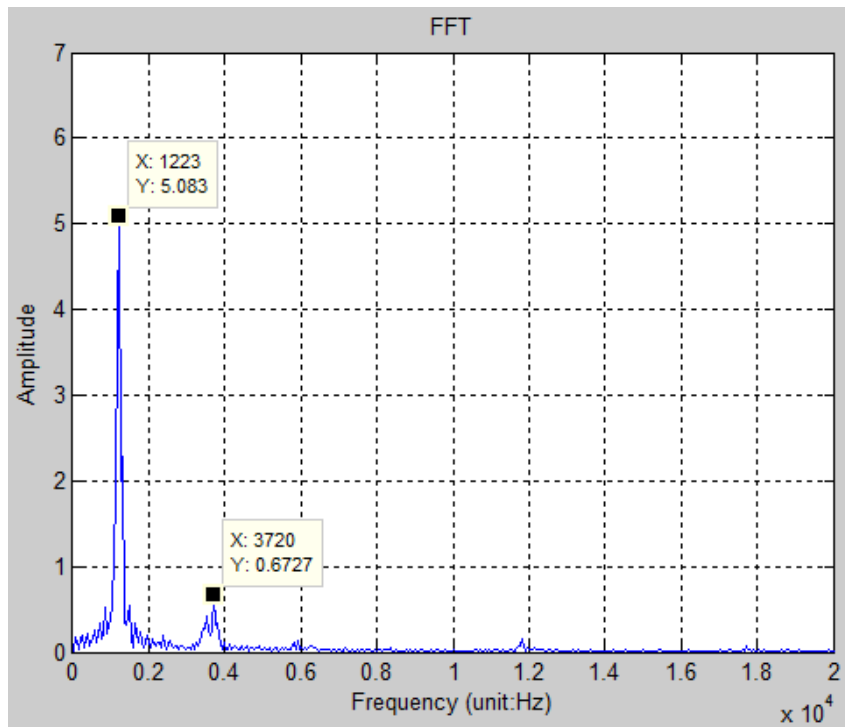
Figure 4b. FFT of noise signal (Set 2)

Figure 5a. Noise signal waveform (Set 3)

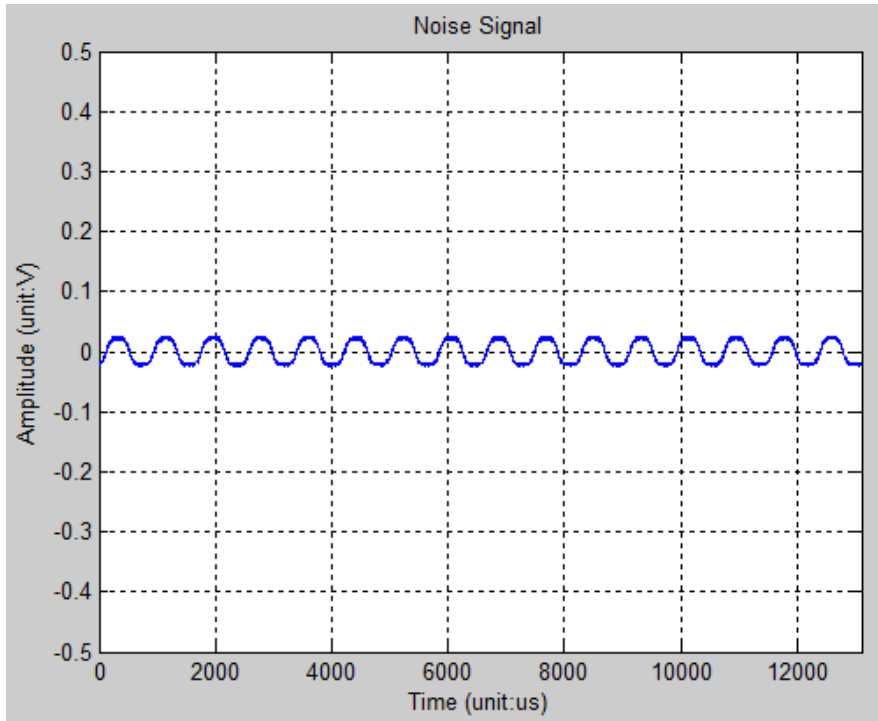Figure 5b. FFT of noise signal (Set 3)

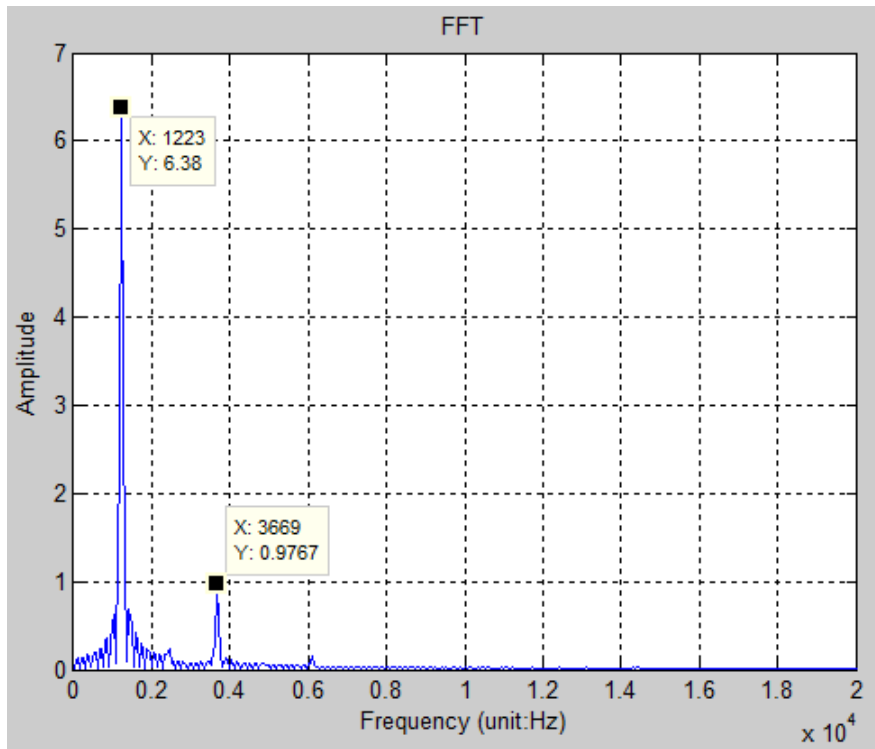Figure 6a. Noise signal waveform (Set 4)

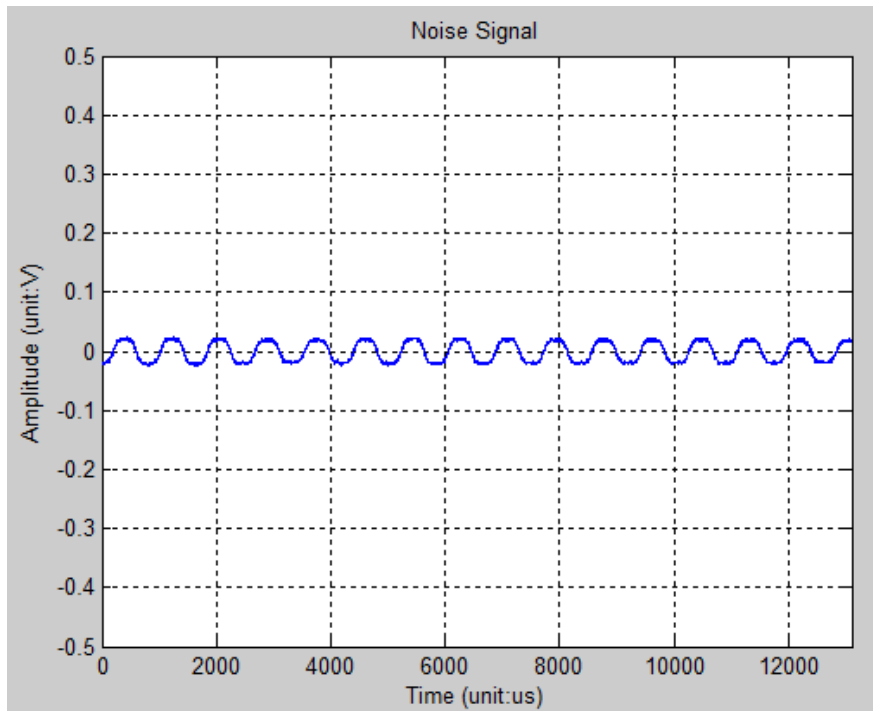Figure 6b. FFT of noise signal (Set 4)
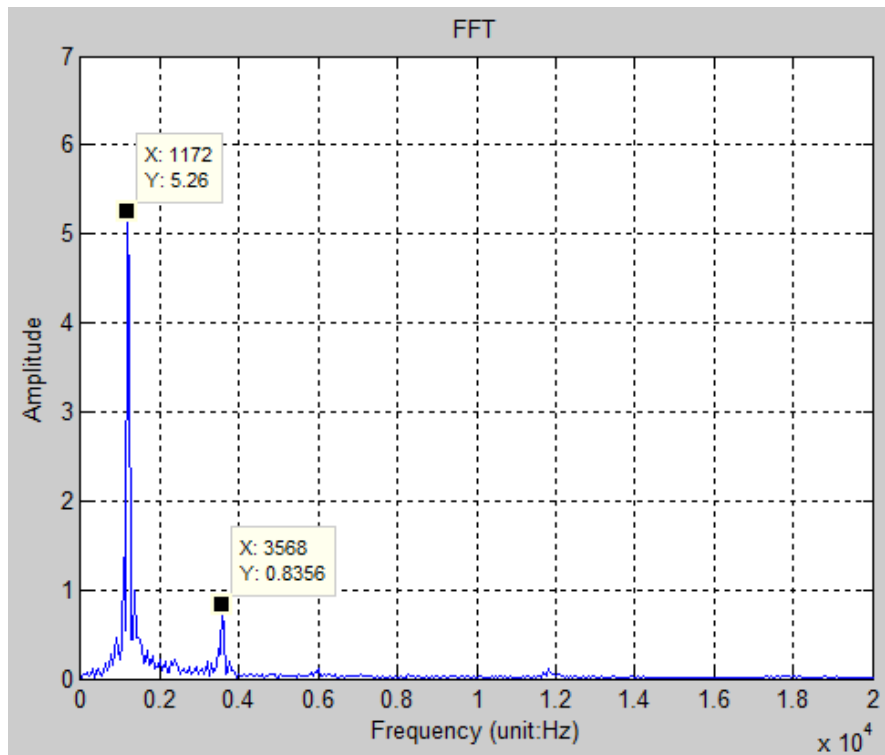
Figure 7a. Noise signal waveform (Set 4)

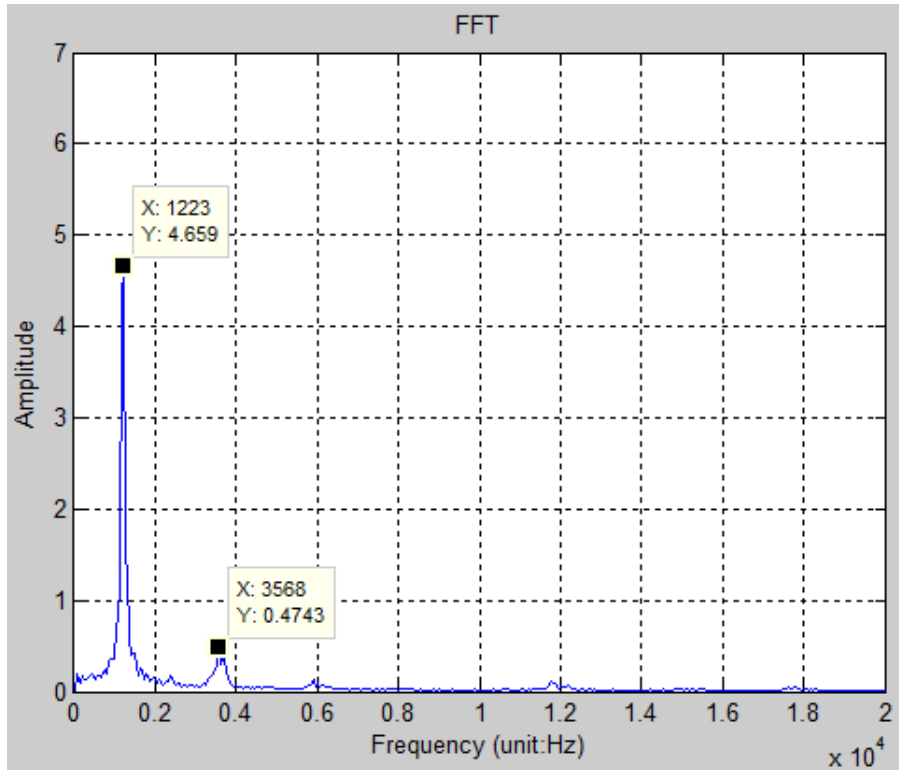Figure 7b. FFT of noise signal (Set 4)

10

Figure 8. Average FFT result of 20 sets noise signal

From the FFT results, we can find that the frequency of the noise signal is around 1.22 KHz.

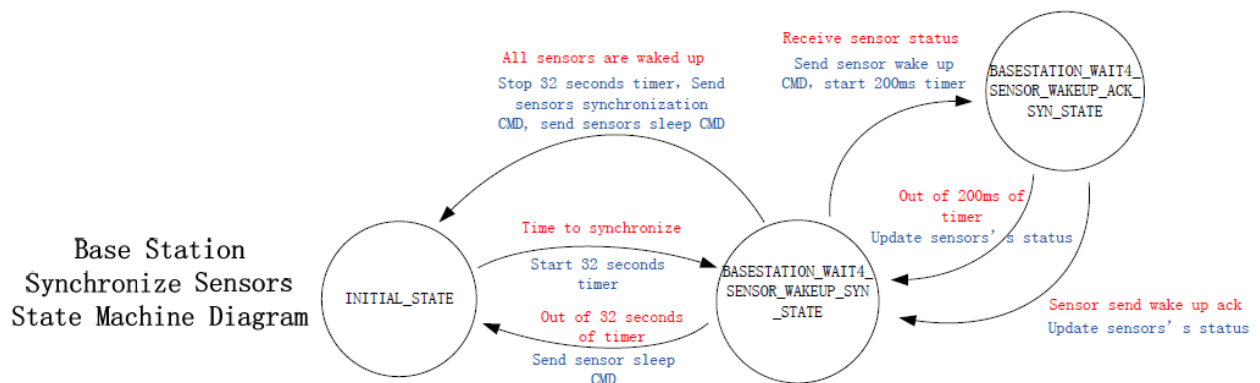2. Optimize and redesign the software structure of the wireless piezoelectric sensor.

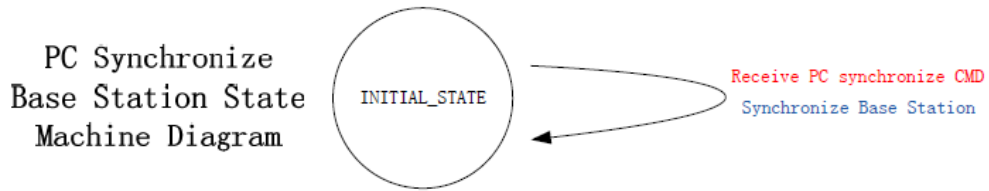Figure 9. Base station synchronize sensors - state machine diagram

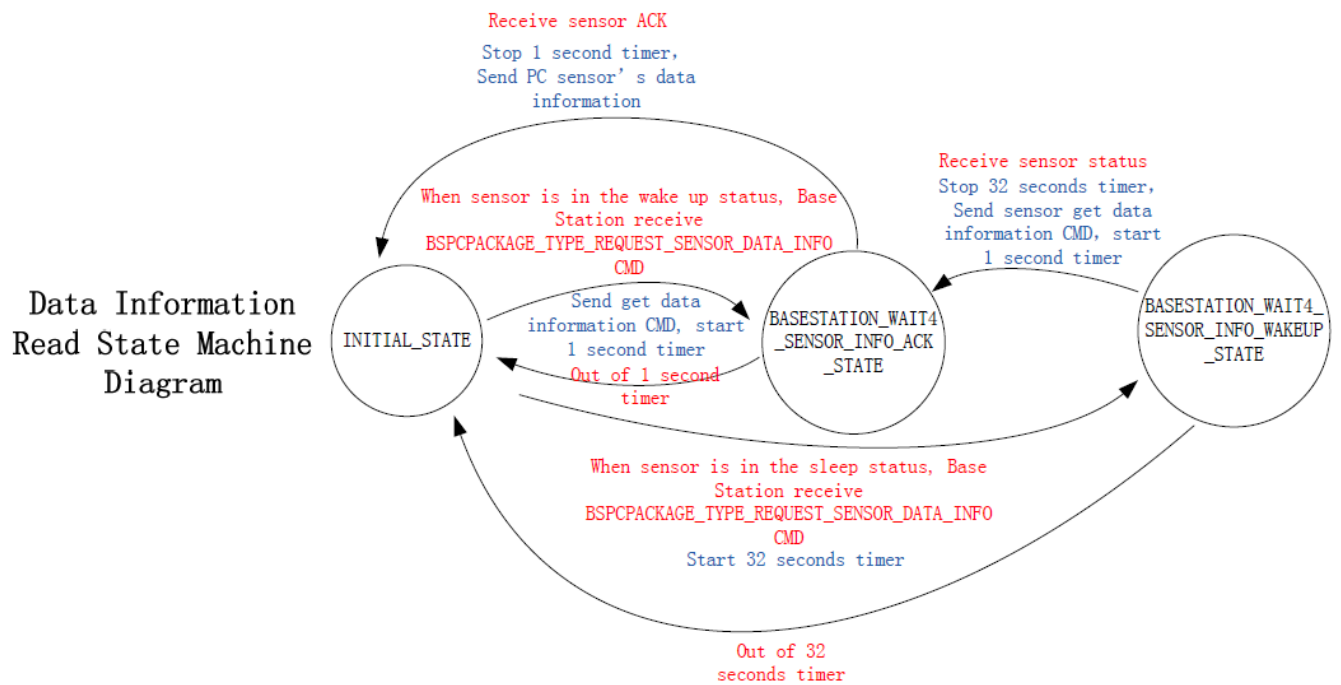Figure 10. PC synchronize base station - state machine diagram

Figure 11. Data information read - state machine diagram
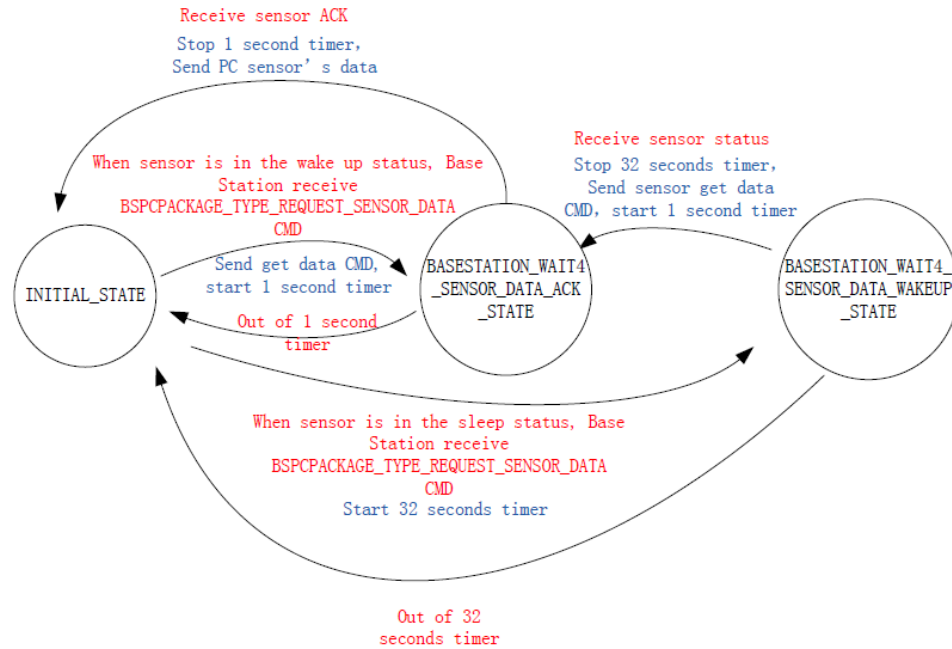
12

Data Read State Machine Diagram

Receive sensor ACK
Stop 1 second timer,
Send PC sensor's data

When sensor is in the wake up status, Base Station receive BSPCPACKAGE_TYPE_REQUEST_SENSOR_DATA CMD

Receive sensor status
Stop 32 seconds timer,
Send sensor get data CMD, start 1 second timer

INITIAL_STATE

Send get data CMD, start 1 second timer

Out of 1 second timer

BASESTATION_WAIT4_SENSOR_DATA_ACK_STATE

BASESTATION_WAIT4_SENSOR_DATA_WAKEUP_STATE

When sensor is in the sleep status, Base Station receive BSPCPACKAGE_TYPE_REQUEST_SENSOR_DATA CMD
Start 32 seconds timer

Out of 32 seconds timer

Figure 12. Data read - state machine diagram

Base Station Acquisition State Machine Diagram

Receive sensor status
Send sensor keep sleep CMD, update sensors' status

Out of 32 seconds of timer
Send sensor sleep CMD, Send PC acquisition failed CMD

Receive Sensor sleep status
Send sensor wake up CMD, Start 200ms timer

BASESTATION_WAIT4_SENSOR_WAKEUP_ACK_STATE

Out of 200ms timer
Update sensors's status

INITIAL_STATE

Receive PC acquisition CMD
Synchronize clock, Start 32 seconds timer

BASESTATION_WAIT4_SENSOR_WAKEUP_STATE

Receive sensor wake up ack
Update sensors's status

All sensors are waked up
Stop 32 seconds timer, Send Sensors acquisition CMD, Start 16 seconds timer

Time to report to PC (Every 16 seconds)
Send all sensors' status to PC, Update sensors' status

Out of 16 seconds of timer
Send sensor acquisition canceled CMD, Send PC acquisition failed CMD

BASESTATION_WAIT4_SENSOR_ACQUISITION_ACK_STATE

Receive sensor acquisition ack
Update sensors's status

Out of acquisition waiting time
Send sensor sleep CMD, Send PC acquisition failed CMD

All sensors finish acquisition
Send PC acquisition finished CMD

All sensors receive acquisition CMD
Stop 16 seconds timer, send PC acquisition start CMD, start acquisition timer

BASESTATION_WAIT4_SENSOR_ACQUISITION_COMPLETED_STATE

Receive sensor acquisition finished ack
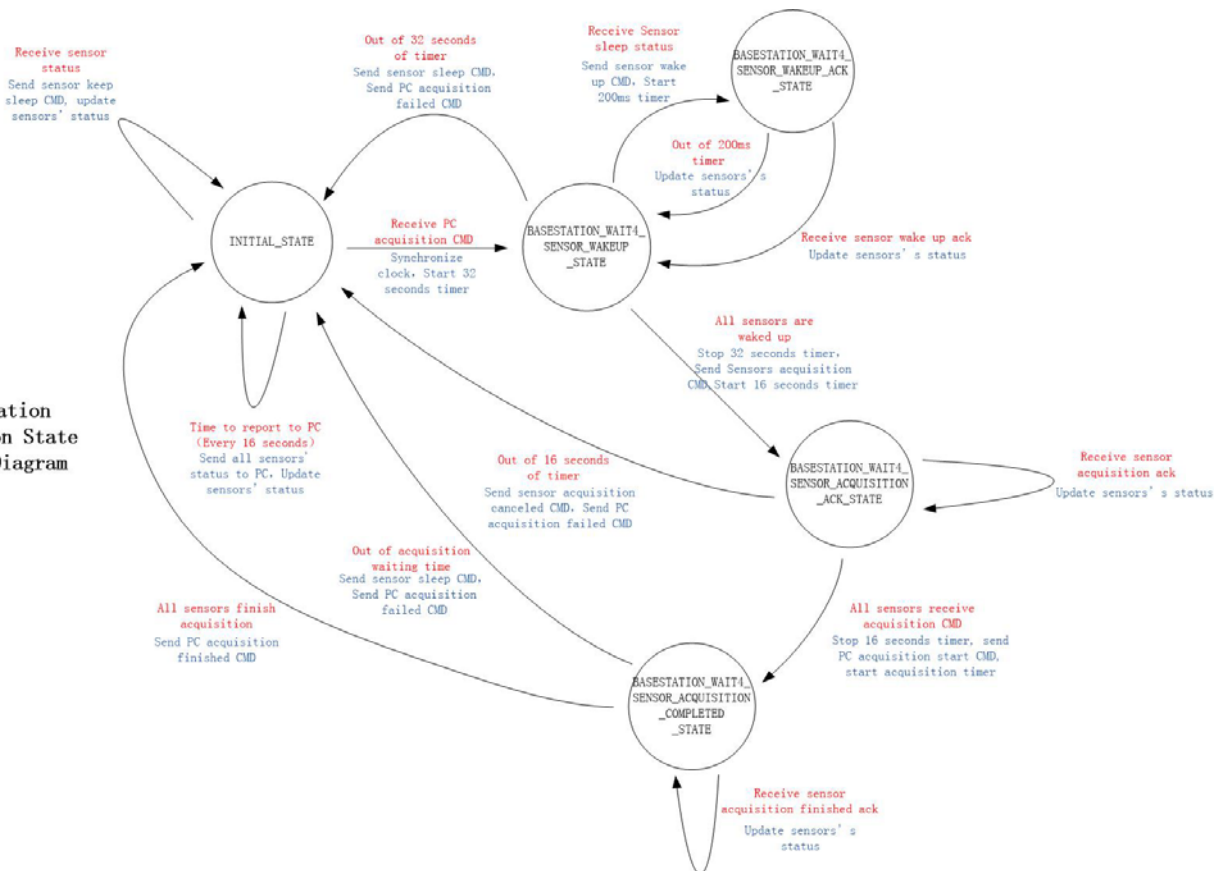Update sensors's status

Figure 13. Base station acquisition - state machine diagram

1.6   Future Plans

Demo Bridge Testing (UMD team led by Dr. Fu) –
- Coordinate with MDSHA on the demo bridge (currently I-95 over Patuxent River was selected) and testing schedule.
- Collecting W-I-M data on I-95 Bridge to simulate traffic through FEM models for all pilot test bridge in Maryland and validating test data with FEM results.
- Establish the local finite element model of the crack location, do the same analysis with the global model, compare the results and discuss the necessarily of local model for our studies.
- Discuss which of the four possible crack configurations has the highest SIF at the crack tip and thus most likely to occur using finite element model.
- Estimate fatigue failure using Wohler Curve (S-N curve) where their results are currently undergoing analysis and comparisons with a probabilistic model for fatigue damage.
- Simplify I270 bridge model dynamic performance for practical consideration
  o Beam model under truck flow
  o Grid model under truck flow

AE Sensor (UMD team led by Dr. Zhang) -
- Field test in March 2014 is planned to test the on-site fatigue crack growth monitoring with wireless piezo film AE sensor and remote sensing features on a steel highway bridge on the Patuxent River along I-95 in Maryland. This bridge is selected to implement full scale integrated structural health monitoring system.
- Data processing and feature analysis of AE signal data recorded from low cycle fatigue loading of steel plate fracture test will be conducted.
- Professional grade piezo film AE sensor will be sent to flexible circuit manufacturer for enhanced weathering and environmental impact protection in February 2014 so they will become ready in the field test. After receiving the orders from the manufacturer, these sensors will be tested first in the lab to characterize its performance for fatigue crack localization.

T-R Method, Energy Harvesting and Smart Sensor (NCSU team led by Dr. Yuan) -
- Finish soldering and preparing all wireless piezoelectric sensors.
- Preparing the 4G gateway and industrial PC.
- Set up the whole wireless piezoelectric system and prepare to install them in the next field test.
- Prepare for Maryland test in March 2014

II — BUSINESS STATUS
- Hours/Effort Expended – As the last reporting period, PI Dr. Fu worked one month paid by his cost sharing account for 167 man-hours. Three (3) UM and two (2) NCSU graduate assistants worked three months half-time (20 hours), the quarterly

accounting deadline, for a total of 1,470 man-hours (one NCSU assistant is partially cost-shared by their University.)

- Total Budget - $1,151,169 & Invoiced (12/31/13) - $898,488 (78%)
- Cost sharing committed - $1,525,063 & Cost shared (7/30/13) - $865,705 (56.8%, will catch up in the next quarter with the support from NCDOT and MDDOT).

ATTACHMENT

**Field Test Status Report
of
MD Bridge No. 1504200 I-270 over Middlebrook Road**

Cooperative Project # RITARS11HUMD
Title: Development of a Self-Sustained Wireless Integrated Structural
Health Monitoring System for Highway Bridges

Between

USDOT Research and Innovative Technology Administration (USDOT/RITA)

and

Maryland Depart of Transportation, State Highway Administration (MDOT/SHA)

From

Chung C. Fu, Ph.D., P.E. and Yunfeng Zhang, Ph.D.
Department of Civil and Environmental Engineering
University of Maryland
College Park, MD 20742

December 2013

Table of Contents

EXECUTIVE SUMMARY

Background

This cooperative project is spsonsored by USDOT Research and Innovative Technology Administration (USDOT/RITA) with in-kind and cash support from University of Maryland, North Carolina State University, Maryland and North Carolina Departments of Transportation where the contribution from Maryland Department of Transportation is in the following areas:

- Participate in the Technical Advisory Committee (TAC, where Mr. Jeff Robert is currently assigned as the liaison)
- Identify and assist on selecting bridge(s) from the Maryland Inventory with fatigue concerns; (With the help from the Remedial Division, The Office of Structures, Dr. Ed Zhou, URS and Dr. C. C. Fu, UMd identified MD Bridge No. 1504200 I-270 over Middlebrook Road as the "Pilot" bridge and a candidate for the final Demo Bridge is I-95 NB/SB Bridge over Patuxent River)
- Assist on collecting information from as-built contract documents, routine and special inspection and inventory data; (Information has been collected for the US1 and I270 Bridges and yet to be collected for the I95 Bridge from The Office of Structures, MDSHA.)
- Provide assistance for field wireless structural monitoring work preparation on the selected bridge(s); (The assistance is listed below)
- Provide assistance for field wireless structural monitoring work preparation on the selected bridge(s); (The assistance is listed below)

Summary of SHA Inpsection Report of I-270 over Middlebrook dated 07/25/2013 on Steel Fatigue Cracks

1) AT GIRDER #3, BAY #2, DIAPHRAGM #3 THERE IS A 2"+- (PREVIOUSLY 1 1/8"+-) LONG, VERY FINE, CRACK IN THE WELD THAT CONNECTS THE WEB STIFFENER TO THE TOP OF THE LOWER FLANGE AT THE SOUTH SIDE OF THE STIFFENER. THE CRACK RUNS ALONG THE TOP OF THE WELD MATERIAL NEXT TO THE STIFFENER AND BEGINS AT THE TOE OF THE WELD, AT THE TOP OF THE LOWER FLANGE. THE OVERALL LENGTH OF THE CRACK IS 2"+- . THERE APPEARS TO BE A 1/4"+- EXTREMELY FINE VERTICAL CRACK AT THE CENTER OF THIS CRACK. THIS CRACK APPEARS TO HAVE GROWN SLIGHTLY INTO THE BASE METAL OF THE STIFFENER.
2) GIRDER #3, BAY #2, DIAPHRAGM #4 HAS A 1 1/2"+- LONG, VERY FINE, CRACK IN THE TOP OF THE SOUTH SIDE WELD. THIS CRACK DOES NOT APPEAR TO HAVE CHANGED.
3) GIRDER #4, BAY #3, DIAPHRAGM #3 HAS A SIMILAR 2"+- LONG (PREVIOUSLY 1 1/2"+- LONG) VERY FINE CRACK IN EACH THE NORTH AND SOUTH, SIDES IN THE TOP OF THE WELD MATERIAL. BOTH OF THESE CRACKS APPEAR TO HAVE GROWN.
4) GIRDER #4, BAY #3, DIAPHRAGM #4 HAS A 1 7/8"+- (PREVIOUSLY 1 1/4"+- LONG) VERY FINE CRACK IN THE TOP OF THE SOUTH SIDE WELD.
5) NONE OF THE PREVIOUSLY MENTIONED CRACKS ARE IN OR NEAR THE GIRDER BASE METAL. ALL OF THE CRACKS ARE IN THE LOWER FLANGE TO STIFFENER WELDS.
6) DIAPHRAGM #3 IS NEAR MID SPAN WHERE THERE IS NOTICEABLE DEFLECTION UNDER HEAVIER LOADS.

Road Field Tests and Visits of I-270 over Middlebrook Road

To monitor the crack growth, three AE sensors were installed on Girder 3 at Girder #3, Bay #2, Diaphragm #3 as described above in item 1), which is the most noticeable cracks of all detected and shown in Figure 4 of Appendix A. Three piezoelectric paint AE sensors were installed on Girder 4 at the other side of Diaphragm #3, as shown in Figure 6 of Appendix A. More details of the instrumentation plan are described in Appendix A.

UMD team has visited the I270 bridges numerous times: one type of visits is with lift truck(s)/MOU provided by the MDSHA and another type is visits without:

A. Field test with the service of lift truck and MOU

1. **March 19 to 21, 2012** - Complete pilot testing was performed on March 19-21, 2012, using AE, accelerometer, deflection and strain sensors for bridge information collection. Stress range records were collected, which will be used as a reference for future testing.
2. **June 28 &29, 2012** - Road testing was again performed, 2012, using deflection sensor for short term and AE and strain sensors for bridge long-term information collection. Longer-term stress range records were collected, which were used as a reference for future testing. Full test was conducted and its FEM analyses of this pilot bridge were performed.
3. **November 15 & 16, 2012** – Visited the field with North Carolina State University team. Replaced one inoperable amplifier with a specialty made amplifier coated with waterproof epoxy. Replaced all sensors and covered with plastic to guard the sensors from moisture. Found there was still interference and brought the PXI back to the lab for more testing.
4. **May 29 & 30, 2013** – Replaced the deteriorated AE sensors and covered them by plastic film to protect them from humidity. Pencil lead break test for calibration and integration with wireless sensors from NCSU was performed. First integration system was field tested.
5. **August 27 2013** – Conducted pencil break tests with new wireless piezoelectric sensor. Due to schedule conflict with Pepco, no real field test with wireless sensors were able to be conducted.

6. **September 26-27, 2013** – Went to the field on September 26th to install wireless sensor and collect 24 hours of data. Removed all testing equipment on the on the 27th.

B. Field test without the service of lift truck and MOU

1. **October 18, 2012** – Checked the connections of Amplifiers, and the DC Power Supply. Reset connections and powered off/on all equipment.
2. **November 2, 2012** – Looked for sources of interference in the field. Brought the PXI system back to the lab. Connected PXI to the laboratory sensors and found the PXI is operating correctly.
3. **November 9, 2012** – Brought the PXI back to the field and attached test panels to compare the plots of sensor data.
4. **November 30, 2012** – Cut wires in 100ft lengths to test if interference was coming from the wires. Consulted with National Instruments (NI) for grounding solutions and for field wiring and noise considerations for analog signals.
5. **December 4, 2012** – Reconfigured the ground so all equipment was grounded to the bridge. This solved the interference problem that was disrupting the AE sensors.
6. **March 13, 2013** – Reset connections and powered off/on all equipment. Reset the AE hardware. Collected all the data from the data acquisition system.
7. **April 19, 2013** – Revisited the bridge to reset the system.
8. **June 19, 2013** – Reset the power system with UBS, the power surge protection and check the sensor functions

Finding of the Field Tests on I-270 over Middlebrook Road

1. Field test on March 19 & 21, 2012 - Field test finding of this trip is contained in Appendix A of this report. This test has collected accumulated AE signals and strain data to check the potential of fatigue growth.

2. Field test on June 28 &29, 2012 - Field test finding of this trip updates the information contained in Appendix A of this report. Samples of Remote Strain Measurement at the Crack Locations for this bridge are listed in Appendix B of the report. The analysis shows that the crack is growing.

3. Field test on November 15 & 16, 2012 - More data of remote strain measurement at the crack locations collected during June to November 2012 are listed in Appendix C of the report. They are listed as AE events and their correspondence with strain gauge data. Appendix D demonstrates traffic loading simulation and bridge finite element analysis to show the local stress contour in graphic form.

4. Field test on May 29 & 30, 2013 - Pencil lead break test for calibration and integration with wireless sensors from NCSU was performed. First integration system was field tested. No real traffic data, just pencil lead break test results are shown in Appendix E.

5. Field test on August 27, 2013 and September 26 to 27, 2013 - During these field tests, existing piezo film AE sensors installed in the late May 2013 were tested with wireless sensor nodes and the pencil break test signals were compared with those collected using wired data acquisition systems. One PZT sensor was found to malfunction in the September field test. Fatigue crack growth
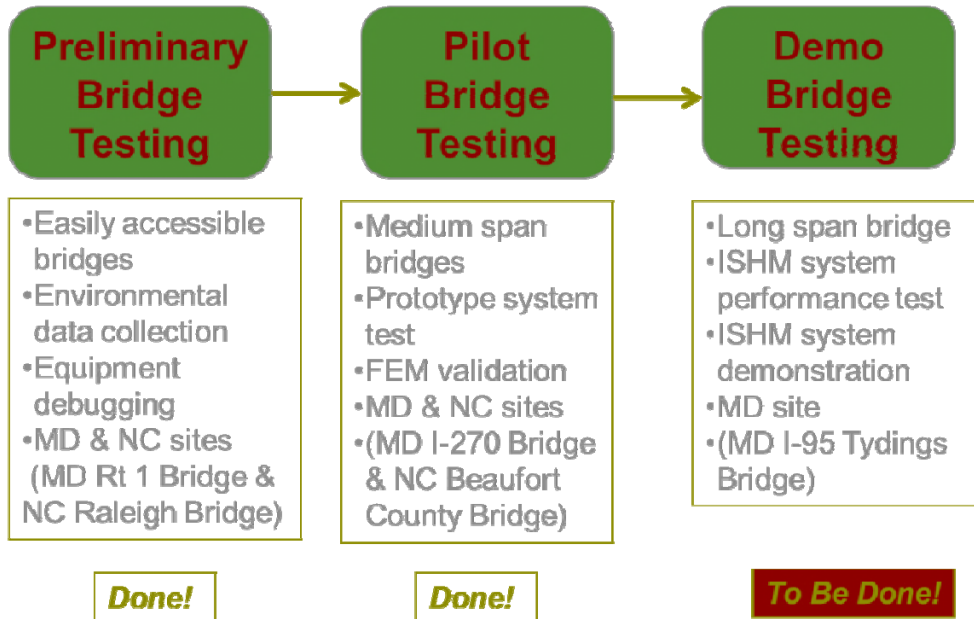
monitoring with piezo film AE sensor was terminated on I-270 bridge on September 27, 2013 and all field test equipment were removed from the bridge.

Conclusion from the Field Tests on I-270 over Middlebrook Road

Analysis of the collected data shows that cracks are growing, but in a very slow pace. Plus, those cracks are located at the secondary load-carrying members so it is not a major concern yet. The wireless Integrated Structural Health Monitoring (ISHM) system has been successfully tested on the "pilot" bridge. We are moving to the next level, the "demo" bridge. For more details and current status of the project, please view our project web site http://www.ishm.umd.edu/.

Summary of Proposed Field Tests

The mission of the field tests listed in the proposal is shown below

Preliminary Bridge Testing	Pilot Bridge Testing	Demo Bridge Testing
•Easily accessible bridges •Environmental data collection •Equipment debugging •MD & NC sites (MD Rt 1 Bridge & NC Raleigh Bridge)	•Medium span bridges •Prototype system test •FEM validation •MD & NC sites •(MD I-270 Bridge & NC Beaufort County Bridge)	•Long span bridge •ISHM system performance test •ISHM system demonstration •MD site •(MD I-95 Tydings Bridge)
Done!	*Done!*	To Be Done!

Preliminary bridge selected is US1 Paint branch Bridge at College Park, which needs no assistance. The mission for the "pilot" bridge, I-270 over Middlebrook Road, as shown above has been accomplished and identified cracks at the connection plates are monitored.

Appendix A - Updated Field Test Report for Bridge No. 1504200 I-270 over Middlebrook Road
By
Dr. Chung C. Fu, PE, and Dr. Yunfeng Zhang

Field test dates: March 19 to 21, 2012
Bridge Type: Single-span composite steel I-girder bridge (span length = 140 ft.; Figure 1)
Location: I-270 (Southbound) over Middlebrook Road near Germantown, Maryland (Figure 2)
Participants:

  UMD Dr. Fu's group: Dr. Chung C. Fu; Graduate Students: Tim Saad and Time Brinner (BDI strain transducer and Cable-Extension Transducer, or called string pot)

  UMD Dr. Zhang's group: Dr. Yunfeng Zhang; Graduate Students: Changjiang Zhou (AE sensor), Linjia Bai (wireless sensor), Zhen Li (laser distance sensor), and Feng Shi (ultrasonic distance sensor)

  URS Dr. Ed Y. Zhou (coordination and oversight)

Figure 1. View of the bridge
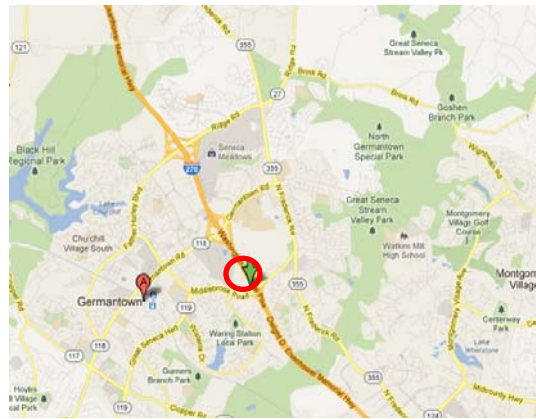
Figure 2. Bridge location (red circle, latitude=39.175296, longitude= -77.247046)

PHASE I – INSTRUMENTATION PLAN

The main data acquisistion (DAQ) systems used in this test are:

  a. PXI-based data acquisition system by National Instruments for data collection from BDI strain transducers, string pots and AE sensors

  b. Multi-channel data acquisition equipment CR5000 manufactured by Campbell Scientific, Inc. for extra BDI strain transducers

Types of sensors used in this project are: 1. piezoelectric paint AE sensors; 2. wireless accelerometers; 3. laser sensor; 4. ultrasonic distance sensors; 5. BDI strain transducers; and 6. String pots.

Instrumentation plan is shown in Figure 3 – Crack locations and sensor placement on the framing plan. Also shown are Figures 4-7 for cracks on Girders 3 & 4 and their respective sensor locations.
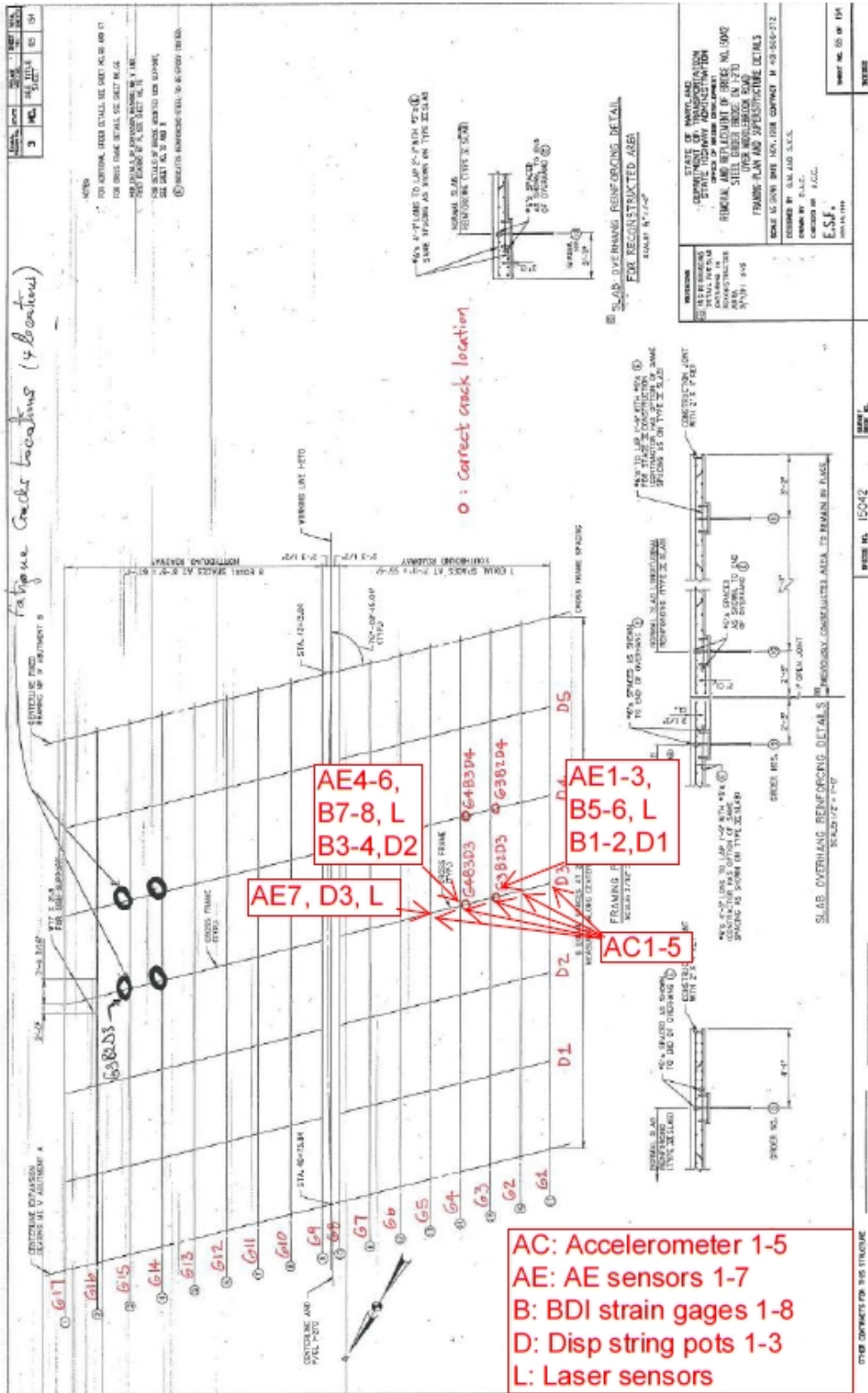
Figure 3 – Crack locations and sensor placement on the framing plan
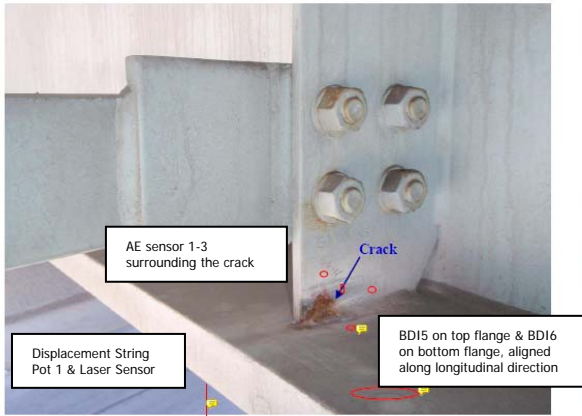
Figure 4. Crack at G3B2D3 (Girder 3 Bay 2 Diaphragm 3) and sensor

Figure 5. No Sign of Cracking at G3B3D3 (Girder 3 Bay 3 Diaphragm 3) and one
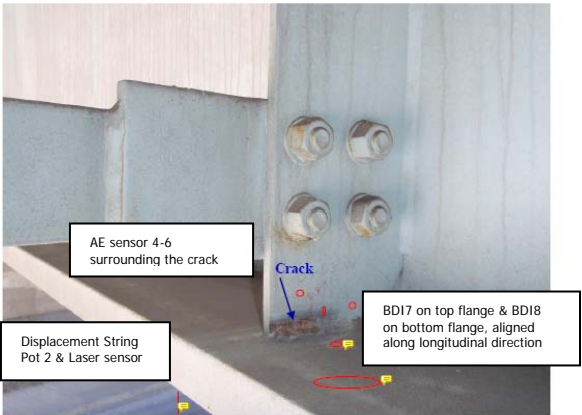
Figure 6. Crack at G4B3D3 (Girder 4 Bay 3 Diaphragm 3) and sensor locations
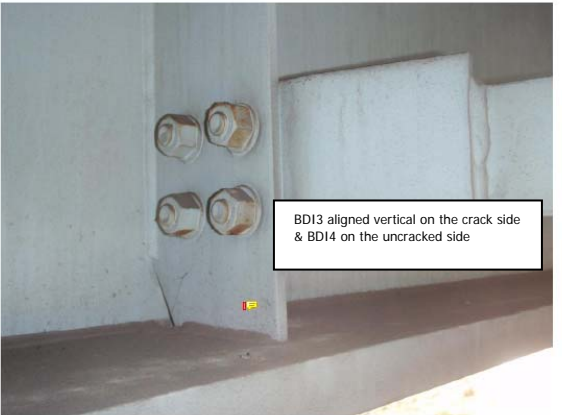
Figure 7. No Sign of Cracking at G4B4D3 (Girder 3 Bay 4 Diaphragm 3) and one sensor

PHASE II – FIELD TEST AND RESULTS

1.   Acoustic Emission Monitoring

A total of seven AE sensors were installed on Girder 3 and Girder 4. Three piezoelectric paint AE sensors were installed on Girder 4. Two of them were placed on the cracked connection plate (see Figure 8) while the third was placed on the uncracked connection plate to provide ambient noise AE data (Figure 9). Figure 10 shows the installation of those AE sensors. Same arrangement is for Girder 3.
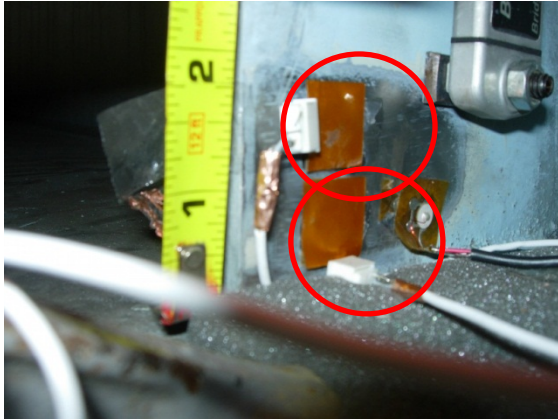
Figure 8. Piezoelectric paint AE sensor on cracked connection plate (red circled, for monitoring fatigue crack in the weld between the connection plate and lower

Figure 9. Piezoelectric paint AE sensor (blue circled, for monitoring ambient noise since there is no fatigue crack on this side connection plate)

(a)

(b)

Figure 10. (a) Installing AE sensors and wiring; (b) AE data acquisition

Installing AE sensors and wiring took quite some time on March 20 and 21, 2012. The first day (March 19) of field test was spent on surface preparation for installing AE sensors and preparing additional preamplifiers for AE sensors. The second day (March 20) was on installing AE sensors and connecting wires and preamplifier for three AE sensors. During the third day (March 21), most of the time was spent on wire connection and debugging the sensors. Data were collected from all seven AE sensors. Continuous AE monitoring was carried out from approximately 1:10pm to 1:55pm on March 21, 2012. Based on past bridge monitoring experience with piezo paint AE sensor and on-site trial on AE data collection, the trigger threshold was set to be 50 mV for each AE sensor channel over this monitoring period (otherwise, if a lower threshold level is used, overly large AE data sets would be collected with much significant AE events), that is, if the AE signal for each chancel exceeds 50 mV, data collection would be triggered and a total of 10,000 data points (5 msec.) will be collected for each channel at a sampling rate of 2 MHz. Over this monitoring period, no fatigue-crack-related AE signal is observed. Samples of AE data and their frequency characteristics (by applying FFT on time series data) are shown in Figure 11. This is probably due to the short AE monitoring period (only 45 minutes) during this field test during which perhaps no heavy loaded trucks crossed the bridge. It is recommended that for the

next field test, a longer monitoring period (e.g., at least three consecutive days) be arranged to collect AE signals related to fatigue crack growth.

(a)

(b)

(c)
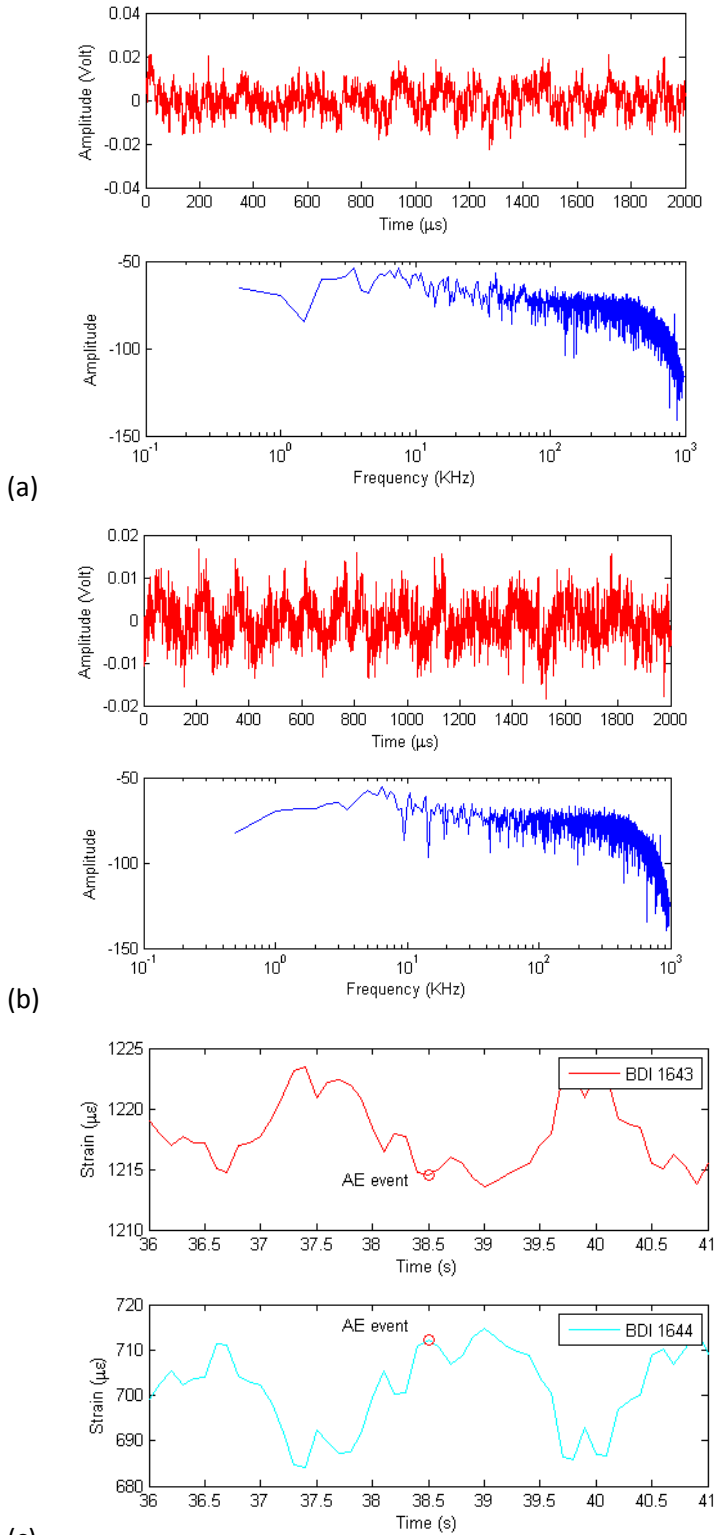
Figure 11. AE data collected by piezo paint AE sensor on Girder 4: (a) ch4 AE data on cracked connection plate; (b) ch6 AE data on uncracked connection plate ; (c) corresponding strain data

25

(from BDI strain gage near ch4 AE sensor), AE data acquired between 38.6 and 38.7 seconds in this figure (highlighted with red circles) (BDI 1643 strain gage on the uncracked side of Girder 4 while BDI 1644 strain gage placed on the cracked side of Girder 4).

2.   Wireless Sensor (monitoring vibration responses of Girders 2 to 5 of the bridge)

A total of four wireless accelerometers (see Figure 12) Imote2 were used to monitor the vibration responses of the bridge. One wireless sensor was installed on one of the girders (Girder 2 to 5) and acceleration data was acquired at 100 Hz sampling rate synchronically. The acceleration data was used to provide modal frequency information (Figure 13) that can be used to calibrate the finite element model of the bridge. The fundamental frequency thus measured is 3.22 Hz, which is very close to the value from finite element analysis (3.14 Hz).

Figure 12. Wireless sensor Imote2 (measuring acceleration and temperature)
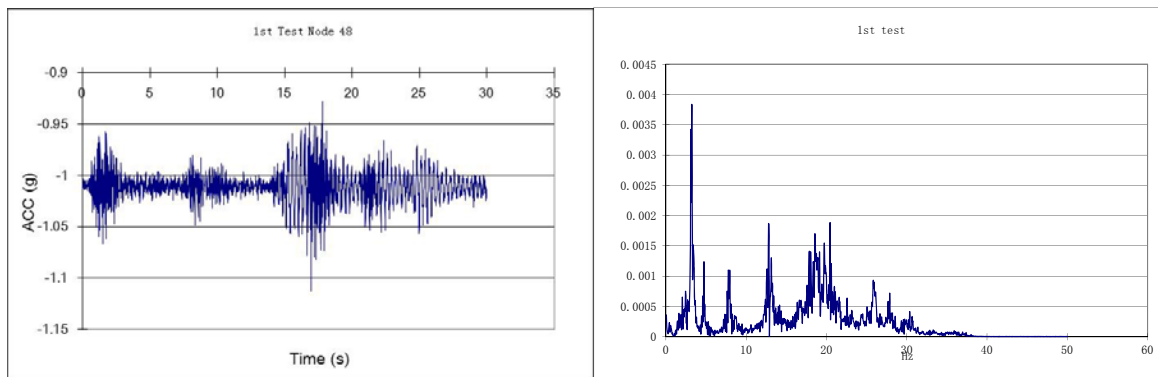
(a) Acceleration time history

(b) FFT of acceleration data (horizontal axis: frequency; vertical axis: FFT amplitude)

Figure 13. Acceleration data measured by wireless sensor

3.   Bridge Deflection Monitoring

Both laser sensor and ultrasonic distance sensors were used to measure the dynamic deflection of the bridge, as shown in Figure 14. Only one laser sensor and one ultrasonic distance sensor were used each

time. The data from laser sensor is shown in Figure 15. The measured deflection value from the laser sensor agrees well with the string pot, and its accuracy is also validated by the fundamental frequency indicated by FFT of the laser sensor measured deflection data (see Figure 16). The ultrasonic sensor data had some problems, most likely due to a high sampling rate (20 Hz seems to be too high for ultrasonic distance sensor of this particular model, next time we will lower the sampling rate to 5 Hz, which provides much better accuracy during lab calibration test) and parasitic echo signals from reflecting background such as lower surface of bridge deck (next field test we will install the ultrasonic distance sensor on the girder and let it shoot down on road surface to avoid background noise).

Table 1. Maximum deflection measured by laser sensor

Girder #	3	4	5
MaxD (m)	0.0066	0.0069	0.0063

Note: MaxD=average(Distance)-minimum(Distance)
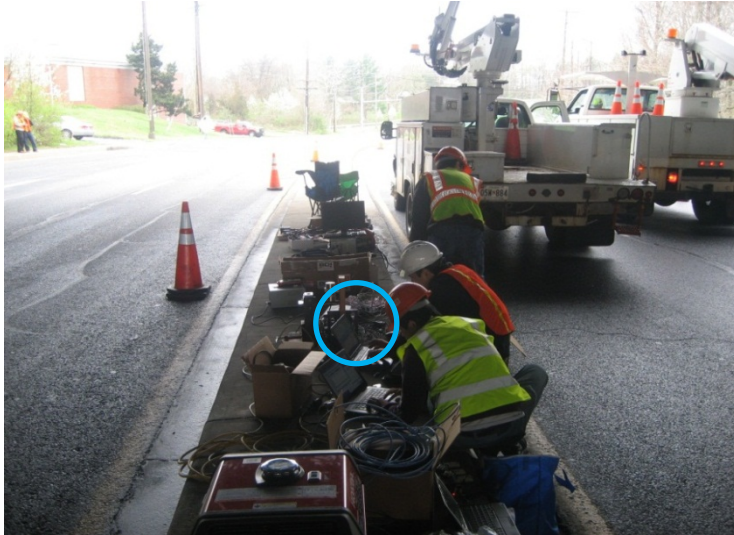
Figure 14. Bridge deflection measurement with ultrasonic distance sensor and laser distance sensor (in blue circle)
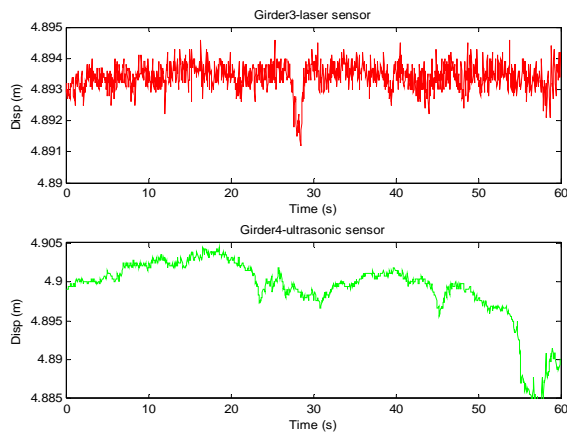
Figure 15. Bridge deflection data by laser sensor (upper) and ultrasonic sensor (lower)
(The measured value is the distance between the sensor and girder bottom surface)
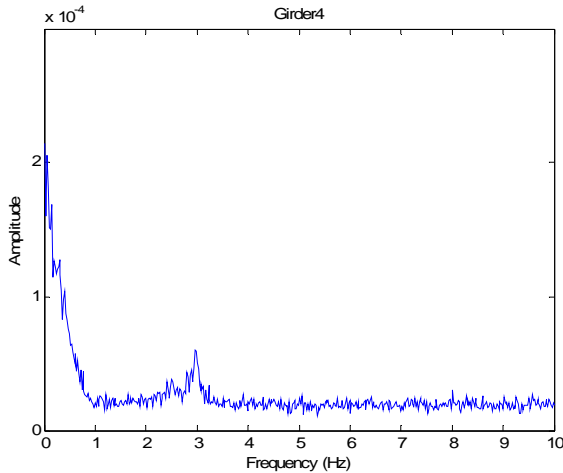
Figure 16. FFT of laser distance sensor
(note the existence of fundamental frequency of the bridge near 3 Hz)

4.   BDI Strain Transducers

BDI 1-4 strain transducers were placed on both sides of the connection plates while BDI 5-8 were placed on the top and bottom flanges on Girders 3 and 4 (Figures 4-7). Since each transducer is unique and individually calibrated, their numbers are marked on Figure 17 for identification. Figures 18 and 19 are showing the measured live load stresses on the flanges and connection plates, respectively.
The maximum longitudinal stress measured on the bottom flange is 1.604 ksi in tension from BDI 3215 on the bottom flange of Girder 3. As for the connection plates, the maximum vertical stresses are 16.18 ksi in tension from BDI 1641 on Girder 3 and 16.1 ksi in tension from BDI 1644 on Girder 4.
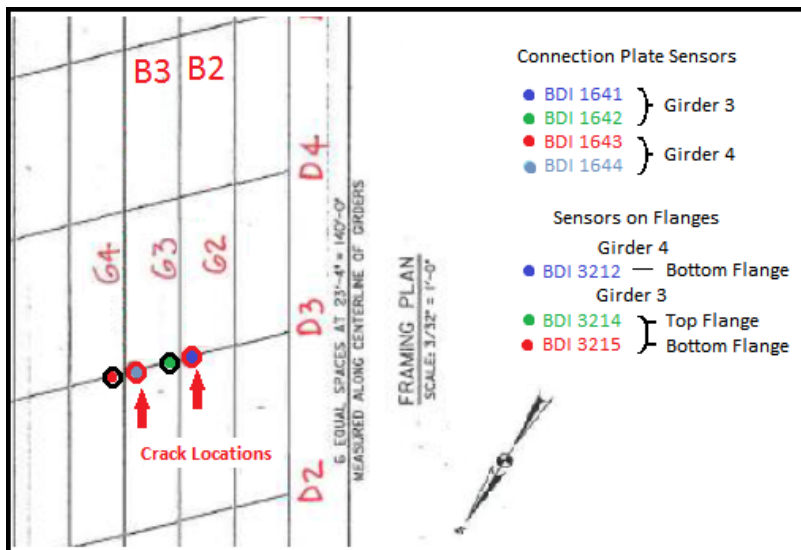
Figure 17. BDI strain transducer locations and marked numbers

28
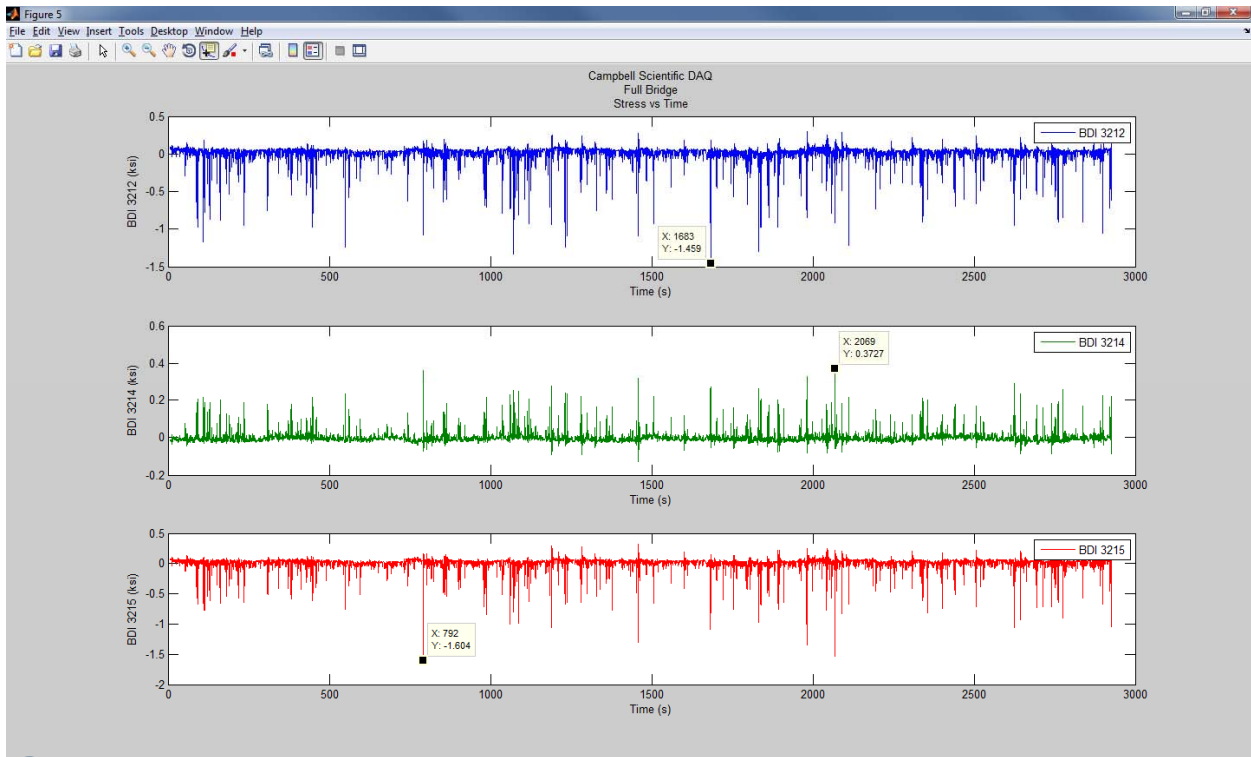
Figure 18. BDI strain transducer flange measurements on Girders 3 and 4
(Positive indicates tension; 3212 G4 bottom flange; 3214 G3 top flange and 3215 G3 bottom flange)
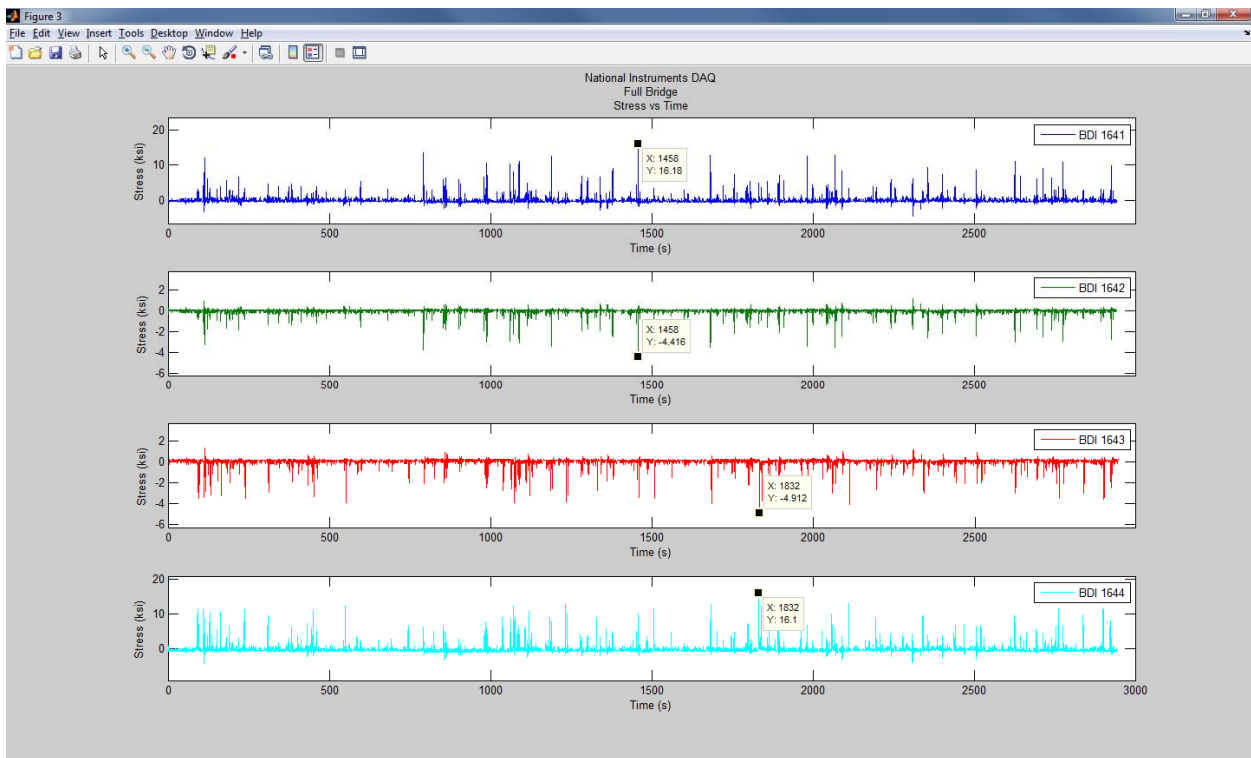
Figure 19. BDI strain transducer connection plate measurements
(Positive indicates tension; 1641 G3 cracked side; 1642 G3 uncracked side, 1643 G4 uncracked side and 1644 G4 cracked side)

5. String Pots

String pots were placed on Girders 3 and 4, synchronized with strain and acoustic emission results. The maximum measurements within the testing period are 0.231" on girder 3 and 0.205" on girder 4, respectively, which are very closed to the laser results, though laser was independently measured. (This short-term measurement is lower than previously measure up to 0.5" or 0.75".)
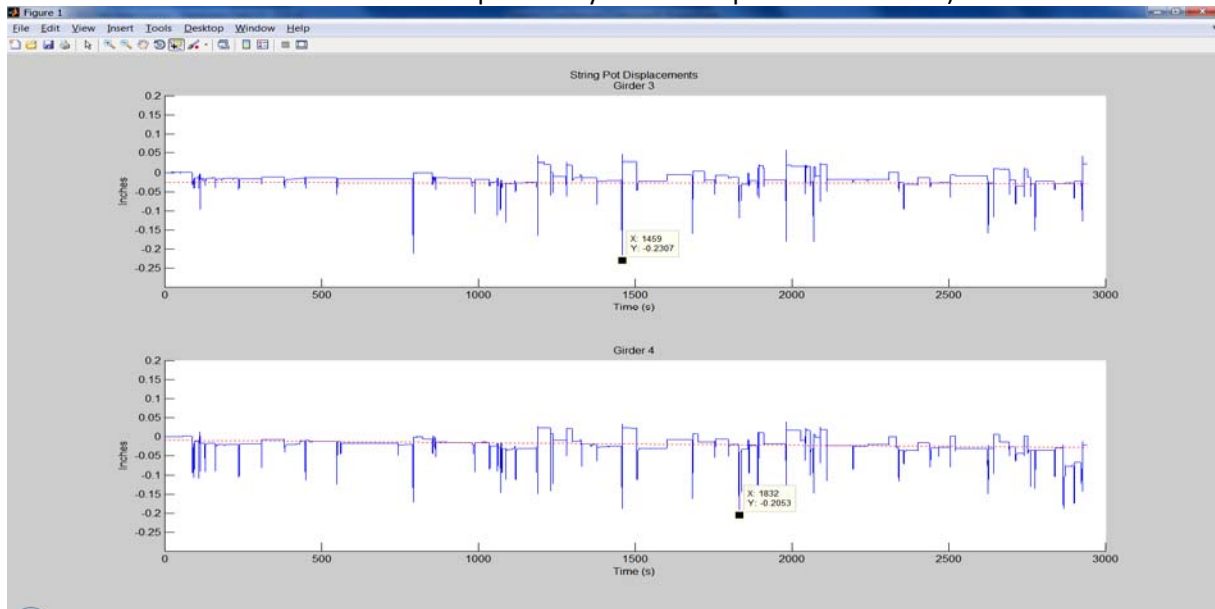
Figure 20. String pot deflection results on girders 3 and 4

PHASE III – FEM ANALYSIS

Finite element model was generated for the bridge. Its model is shown in Figure 21 and its first natural frequency is calculated around 3.11 for a fixed-fixed boundary condition and lower for the normal analysis of fixed-free boundary condition. This is a skewed bridge and the x-translational direction is along the longitudinal direction of the bridge. Fixed-fixed boundary condition represents all x-, y- and z-translational degrees-of-freedom of the five nodes at the bottom flange for each girder on both ends are fixed while fixed-free boundary condition represents x-translational degree-of-freedom of one end is freed (as a roller end). For comparing the first mode, fixed-fixed condition is more realistic where the test result is 3.22 Hz and FEM result for fixed-fixed condition is 3.14 Hz (Table 2).

30
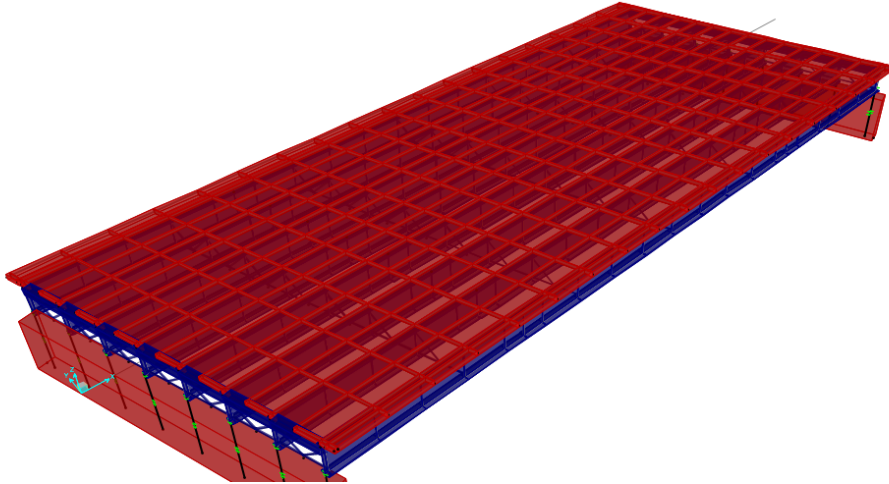
Figure 21. FEM model of the Middlebrook Road Southbound Bridge by CSI Bridge
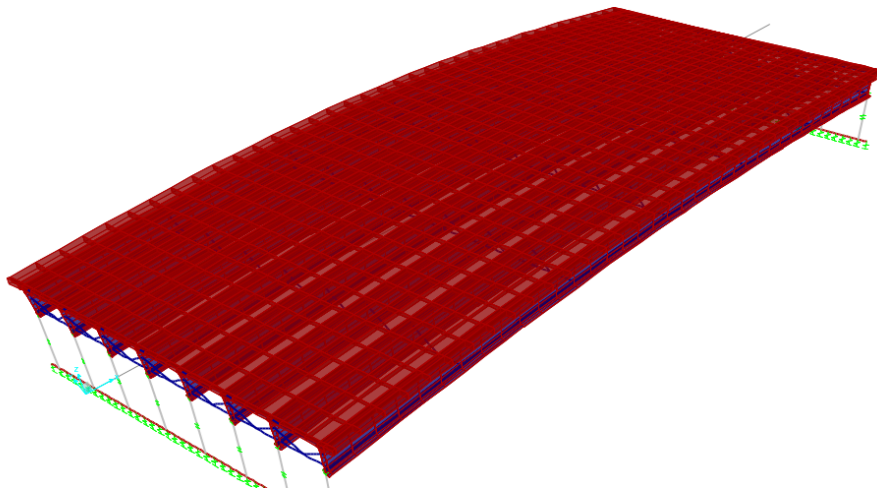
Figure 22. Modal shape of the first mode (f = 3.136 Hz) by CSI Bridge

Table 2 – Natural frequencies by FEM analysis

Hz	Fixed-Fixed	Fixed-Free
1	3.136131	2.235395
2	3.204958	2.730252
3	5.483081	5.030165
4	5.581643	5.16084
5	6.518478	6.48045

To simulate the traffic, Weigh-in-Motion data was collected from the Hyattstown southbound station, which is located on I270 about 10 miles north of the tested bridge. A more accurate simulation process is still under development. In order to get approximate traffic loading, seven cases of HS-20 truck loading with run stream on different lanes of different patterns were simulated which are:

Case 1: 3 trucks passed the bridge one by one (one at a time) in different lanes

Case 2: the 3rd truck entered the bridge when the 1st truck just left the bridge (only two trucks on the bridge at the same time)
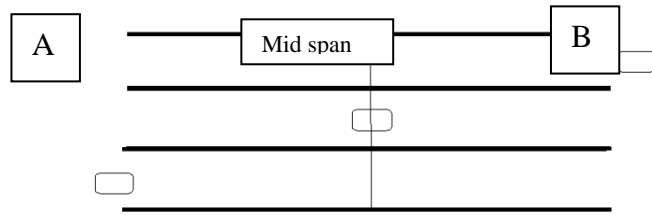
A   Mid span   B

Case 3: the 3rd truck entered the bridge when the 1st truck and 2nd truck just left mid span
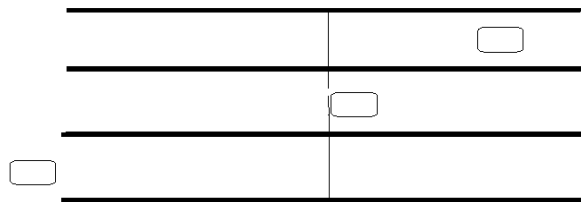
Case 4: the 1st truck left the bridge when the 2nd truck and 3rd truck just entered the right span one after the other
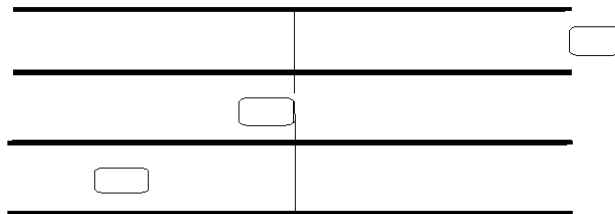
Case 5: the 1st truck and the 2nd truck passed the bridge parallel
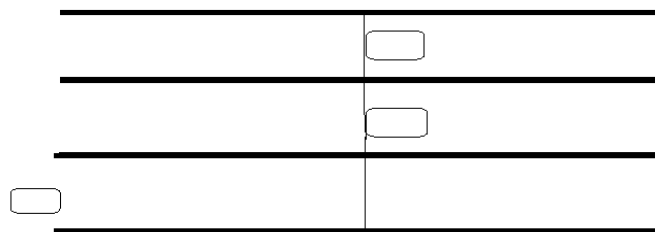
Case 6: the 1st truck just left when the 2nd & 3rd truck is @ mid span
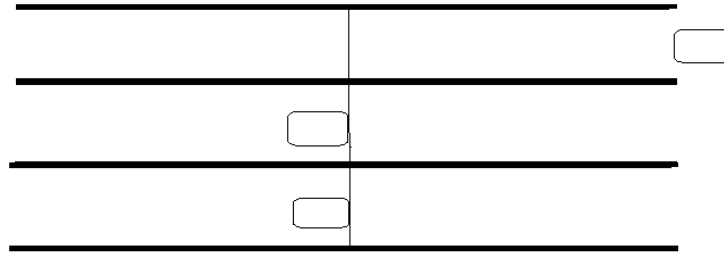
Case 7: 3 trucks passed the bridge at the same time, no truck load reduction is applied
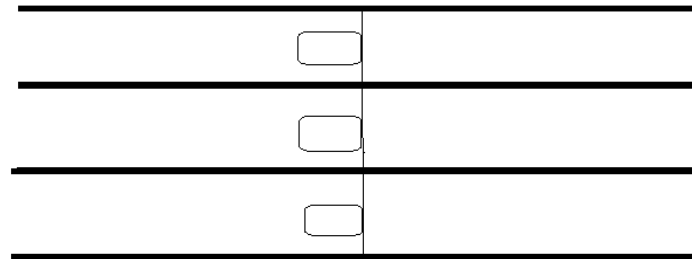
Table 3 – Maximum bottom flange stress ranges of seven truck simulation cases

	GIRDER3	GIRDER4
LL_CASE	ksi	ksi
CASE1	1.229	1.281
CASE2	1.249	1.343
CASE3	1.239	1.281
CASE4	1.507	1.486
CASE5	1.189	1.316
CASE6	1.926	2.128
CASE7	2.245	2.369

Since this is a simple-span bridge, the maximum stress ranges at the bottom flange are close to the maximum stresses, which are demonstrated in Figure 18. The maximum stress measured on the bottom flange of girder 3 is 1.604 ksi where the FEM maximum stress ranges for case 4 for two HS-20 loaded subsequently on two near lanes is 1.507 ksi and case 6 for two HS-20 loaded on two near lanes is 1.926 ksi, respectively. Case 7 for three lane lsimultaneously loaded, based on AASHTO LRFD Specifications that can be reduced by a multiple presence factor of 0.85, yields 1.908 ksi (0.85*2.245 ksi). Global tress contour and its close-up view (in kips/ft2; divided by 144 to convert the scale to ksi) are shown in Figure 23 (a) and (b). Due to program limitation, the connection plates were not modeled.
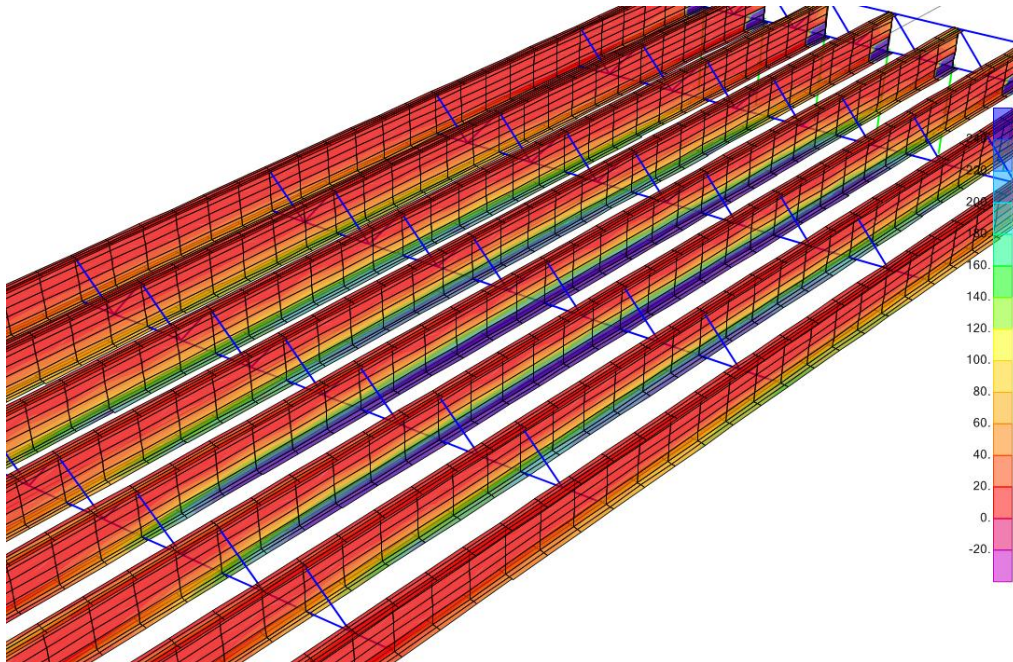
(a) Global stress contour (in kips/ft2) of eight southbound girders (looking south)
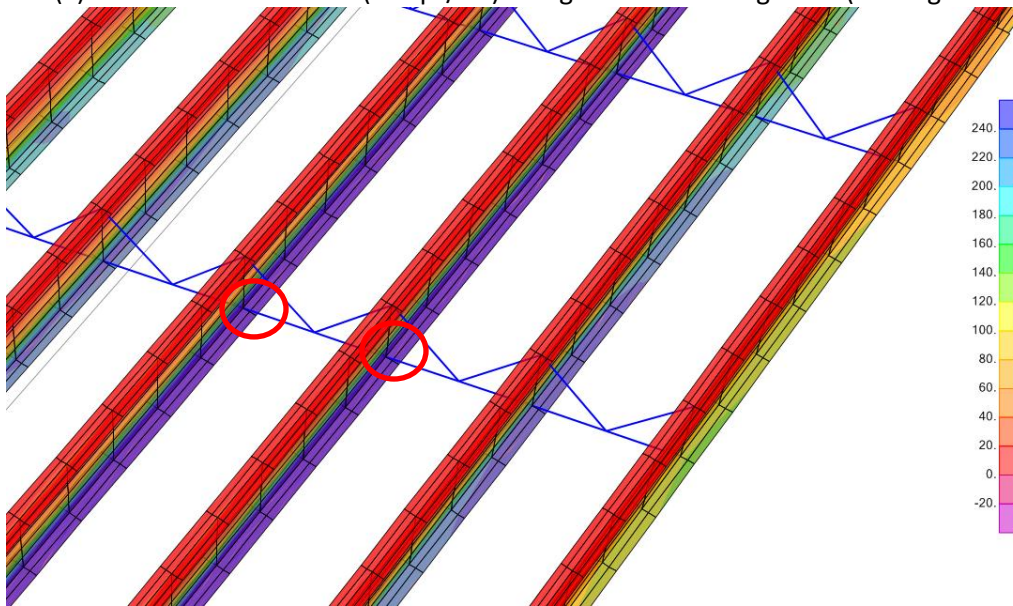
(b) Close-up view of girders 3 and 4 with fatigue cracks

Figure 23. Live load stress contour of truck loading case 6

High tension stress on the connection plates on Girders 3 and 4
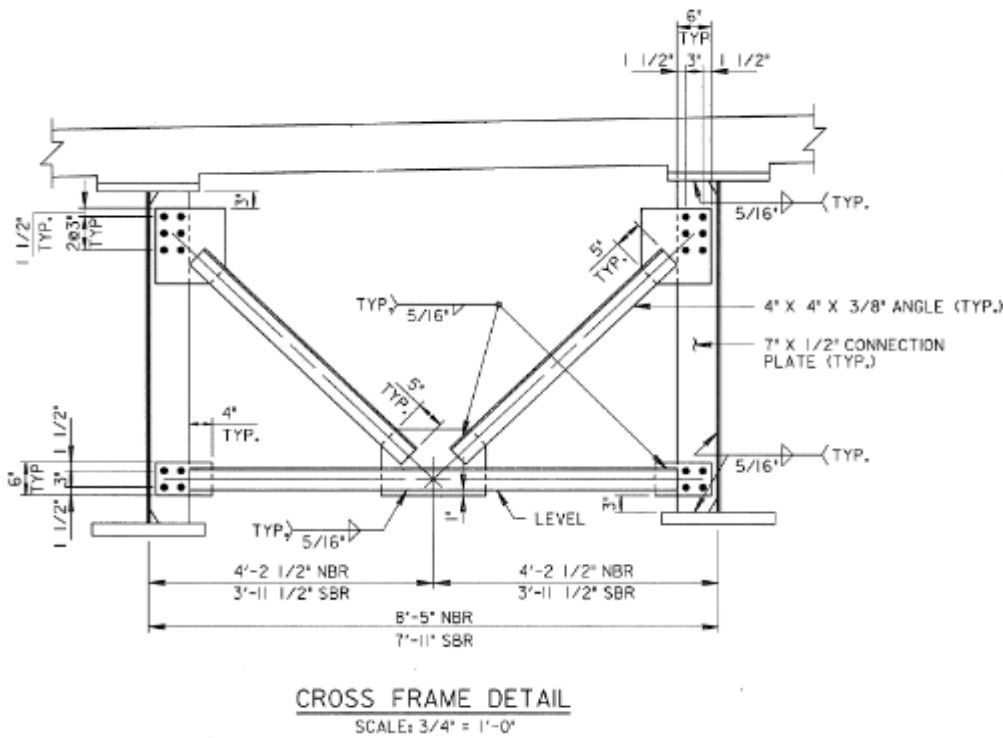
Figure 24. Typical cross frame detail

Out of all types of cross-frames, X-type with top and bottom chords is the stiffest of all, then the K-type with top and bottom chords, then the X-type with bottom only and the flexible one is the K-type with bottom chord only. Differential displacement between girders will cause one diagonal in tension and one in compression. Since the working point of the diagonal is not at the junction of girder web and top flange plus no help from the top chord, one side of the connection plate will be under tension and one under compression. Measured 16.1 ksi in tension is not surprising with the flexibility of the cross-frame and the girder system (with up to 0.5" to 0.75" vertical deflections due to live load observed.)

Figure 25 shows the numbering for the cross-frames near the crack locations.   Table shows their corresponding forces.
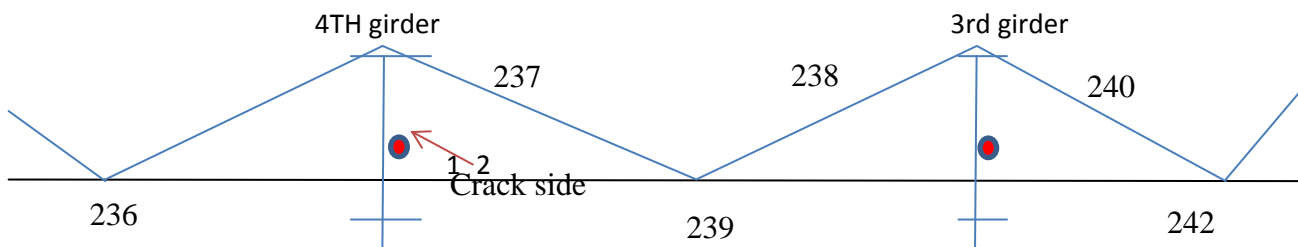
Figure 25. FEM numbering for the cross-frames near the crack locations

Table 4. Cross-frame maximum envelop element forces of seven simulated live load cases

35

Max. Envelop		P (kip) for #236		P (kip) for #239		P (kip) for #242	
	Element	Tension	Comp	Tension	Comp	Tension	Comp
CAES1_LL	1	13.37	-0.94	15.42	-0.23	13.58	-1.37
	2	15.39	-0.23	13.56	-1.41	8.33	-1.18
CASE2_LL	1	13.55	-0.45	16.14	-0.13	14.32	-1.30
	2	16.10	-0.14	14.28	-1.30	8.61	-1.15
CASE3_LL	1	10.69	-0.85	6.21	-0.24	13.69	-1.43
	2	6.24	-0.26	13.66	-1.45	8.33	-1.27
CASE4_LL	1	20.35	-0.88	17.42	-0.21	13.66	-0.26
	2	17.41	-0.23	13.64	-0.28	8.36	-0.23
CASE5_LL	1	22.19	-0.95	16.79	-0.15	14.58	-0.15
	2	16.74	-0.17	14.56	-0.17	8.39	-0.18
CASE6_LL	1	13.39	-0.13	21.23	-0.17	19.70	-1.14
	2	21.23	-0.17	19.63	-1.16	9.13	-1.06
CASE7_LL	1	21.36	-0.22	21.58	-0.26	18.16	-0.30
	2	21.56	-0.26	18.09	-0.31	8.08	-0.18

	P (kip) for #237		P (kip) for #238		P (kip) for #240	
	Tension	Comp	Tension	Comp	Tension	Comp
CAES1_LL	5.756	-6.606	6.612	-5.741	0.174	-3.62
CASE2_LL	5.524	-6.815	6.816	-5.507	0.106	-3.933
CASE3_LL	5.589	-2.65	2.649	-5.574	0.162	-3.696
CASE4_LL	5.731	-8.317	8.323	-5.712	0.163	-3.648
CASE5_LL	5.686	-8.125	8.136	-5.676	0.083	-4.269
CASE6_LL	0.1	-2.391	2.402	-0.101	0.085	-7.468
CASE7_LL	0.076	-3.008	3.028	-0.083	0.101	-6.957

In order to maximize the differential displacement and bracing elements, two more loading cases to simulate more truck traffics and field measured stresses are added to the run:

Case 16: the 1st group trucks passed the bridge side-by-side on fast lanes and 2nd group 25' behind
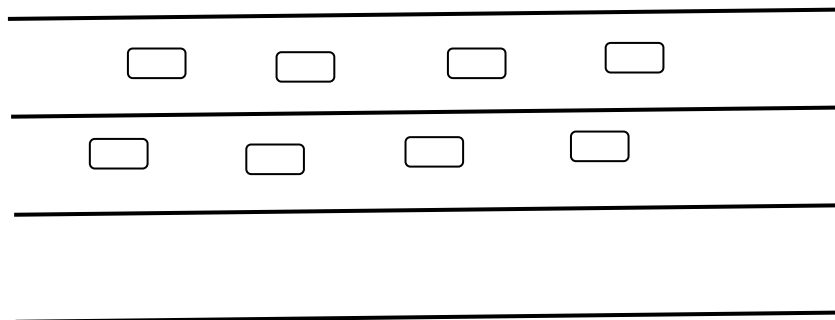
Case 17: the 1st group trucks passed the bridge side-by-side on slow lanes and 2nd group 25' behind
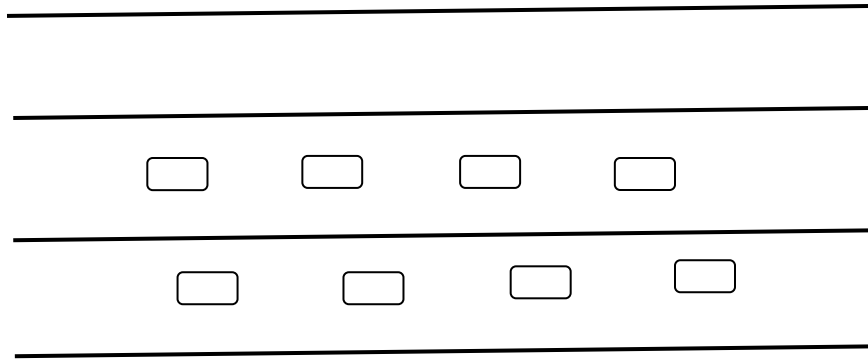
Max. stress	girder 3 crack location connected with the bottom chord between girder 2 and 3	girder 4 crack location connected with the bottom chord between girder 3 and 4
case 16_LL	**7.32ksi**	**17.95ksi**
case 17_LL	19.59ksi	21.68ksi

Maximum differential displacement of -0.316584 inches is found between girders 2 and 3 under live load case 16 (-0.303624 inches between girders 3 and 4).
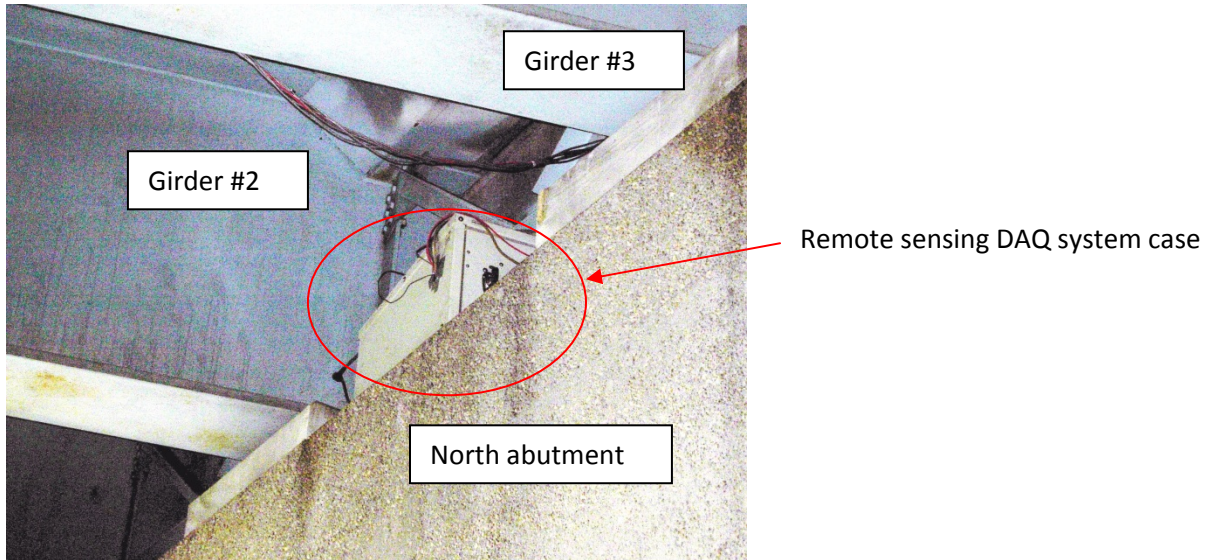
Figure 1 – Case containing remote sensing DAQ system on the top of the bridge pier
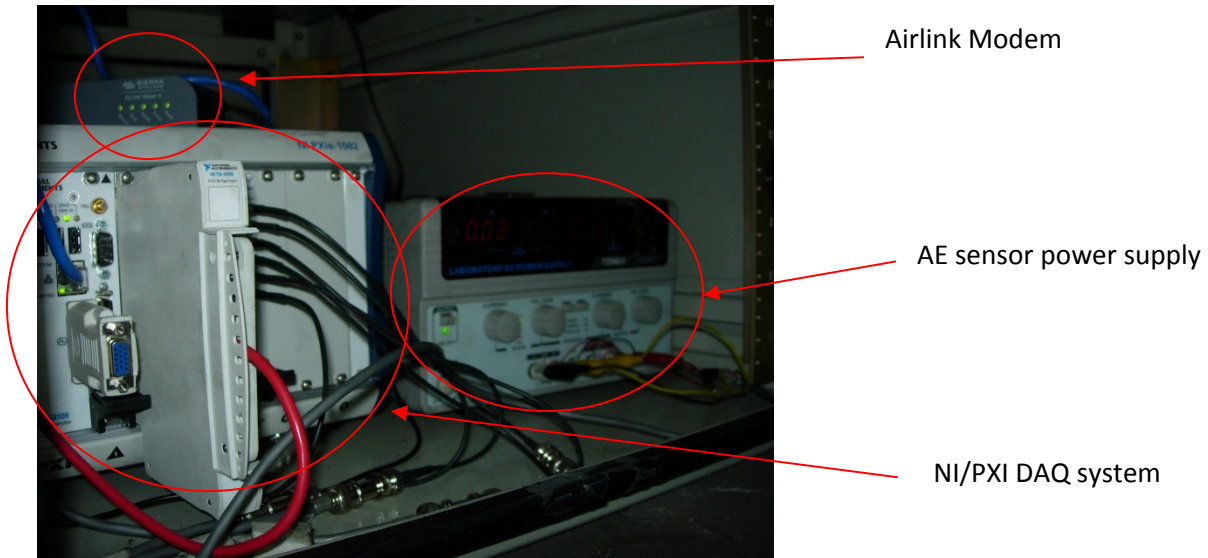
Figure 2 – Close look of the remote sensing DAQ system inside the case
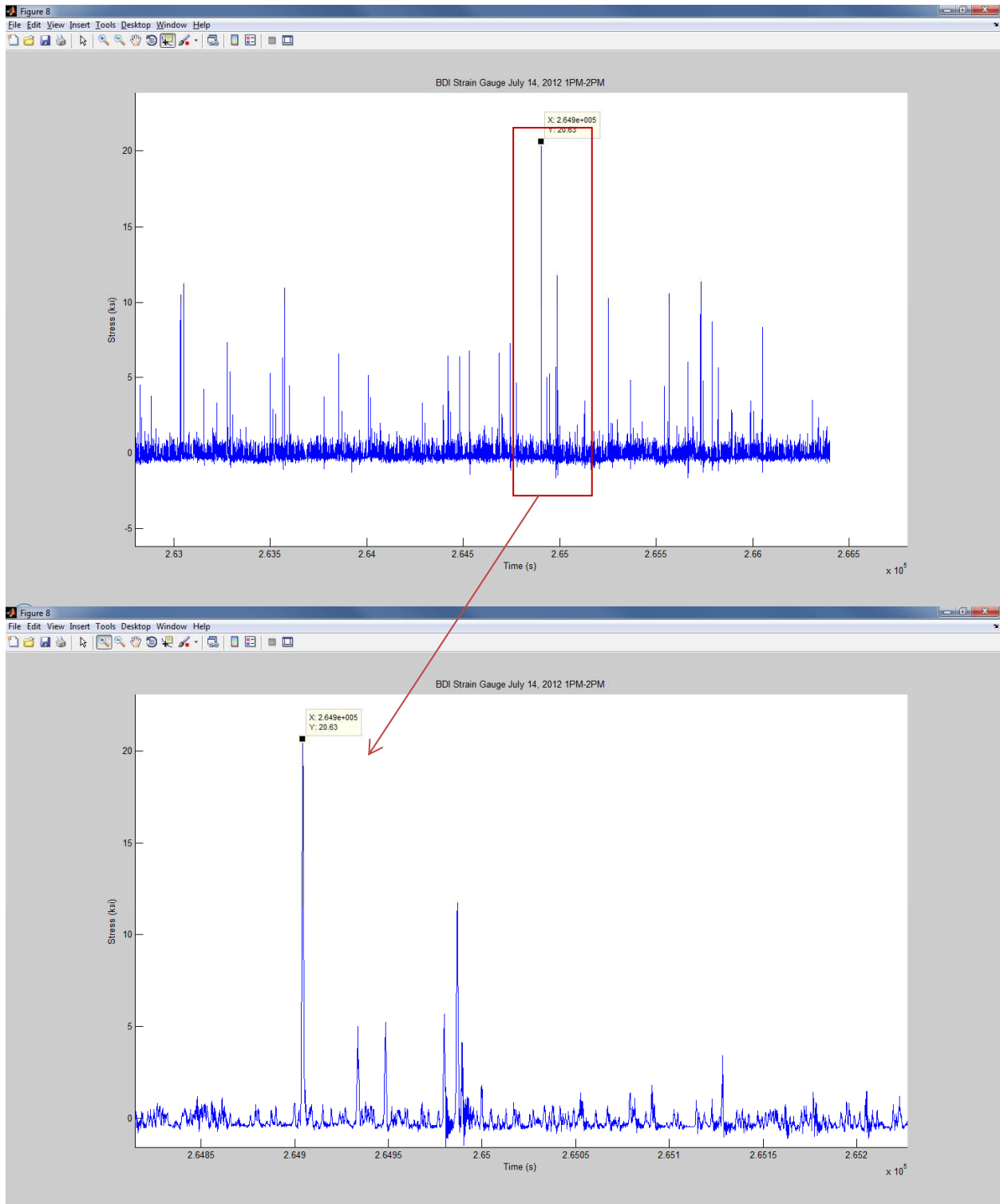
Figure 3 – Sample segment 1 of the continuously monitored strain data
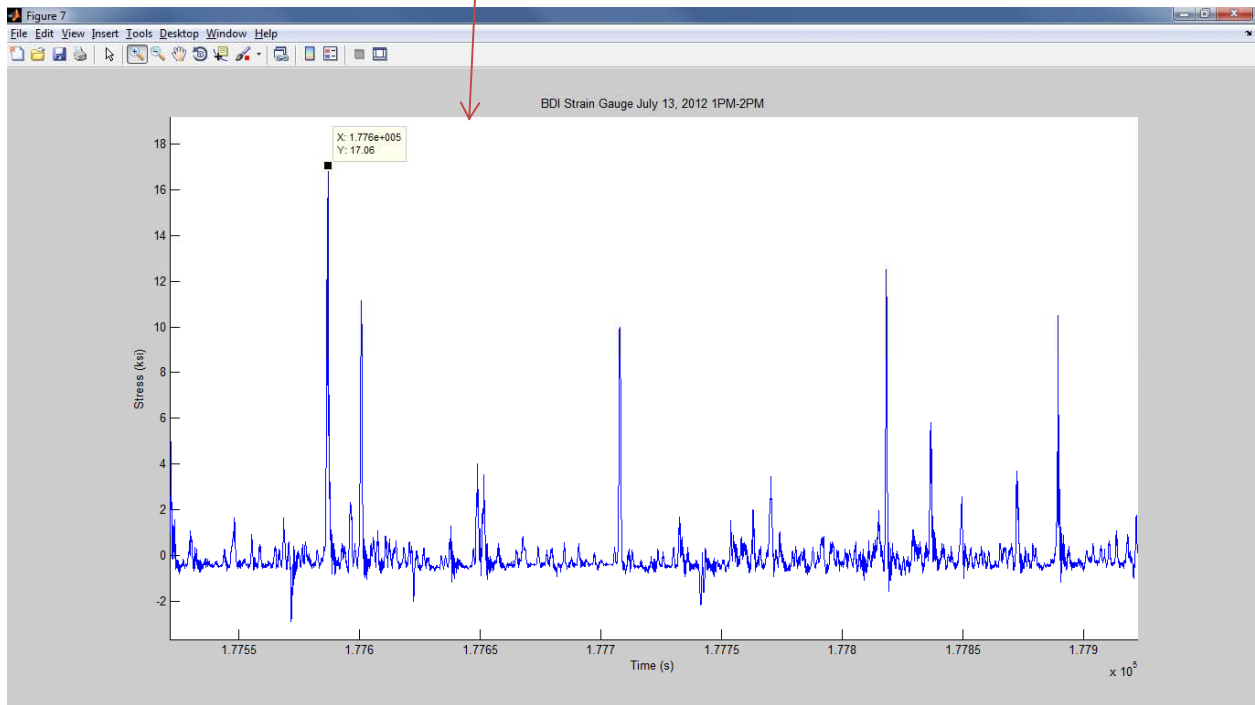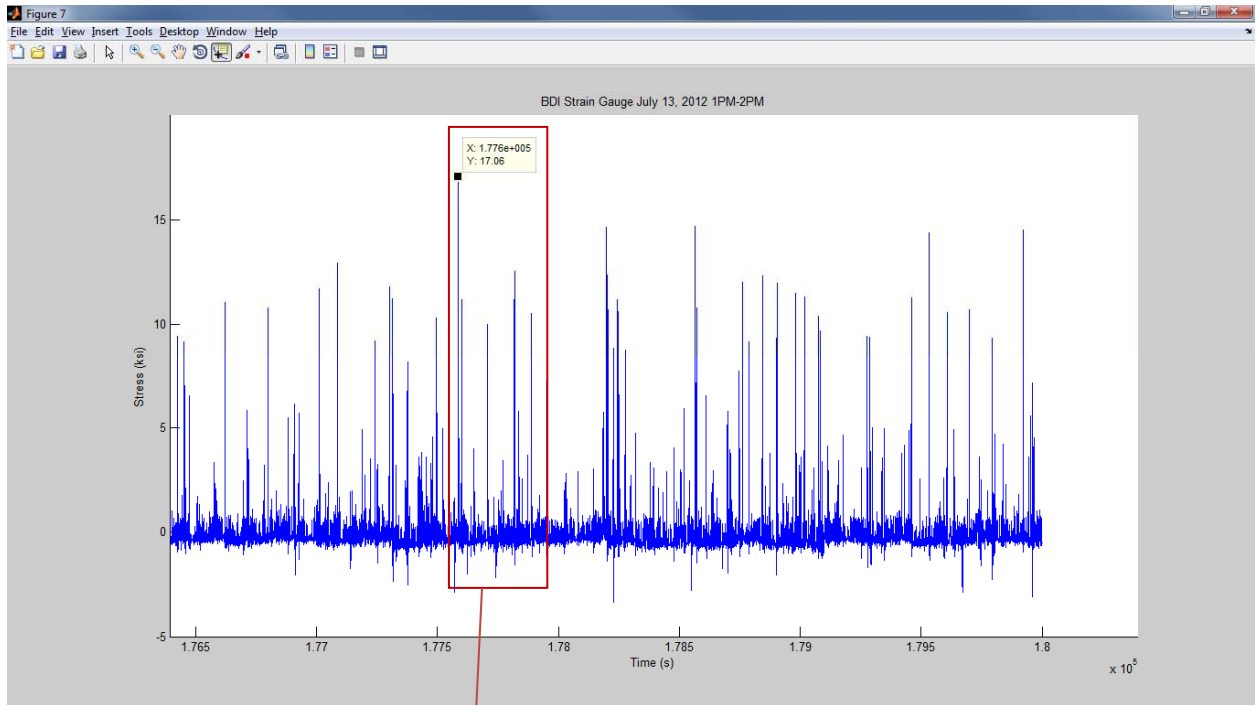
Figure 4 – Sample segment 2 of the continuously monitored strain data
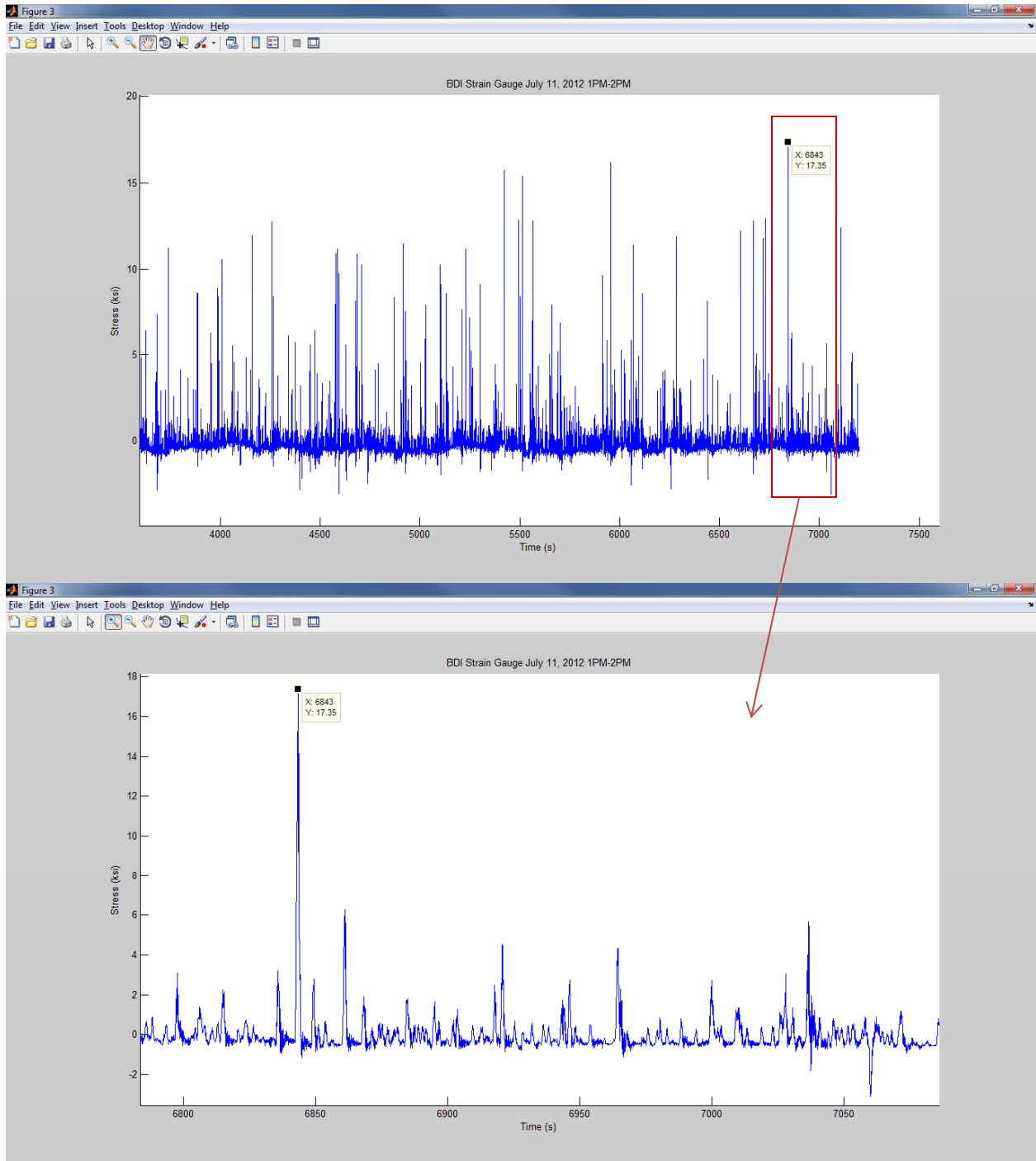
Figure 5 – Sample segment 3 of the continuously monitored strain data
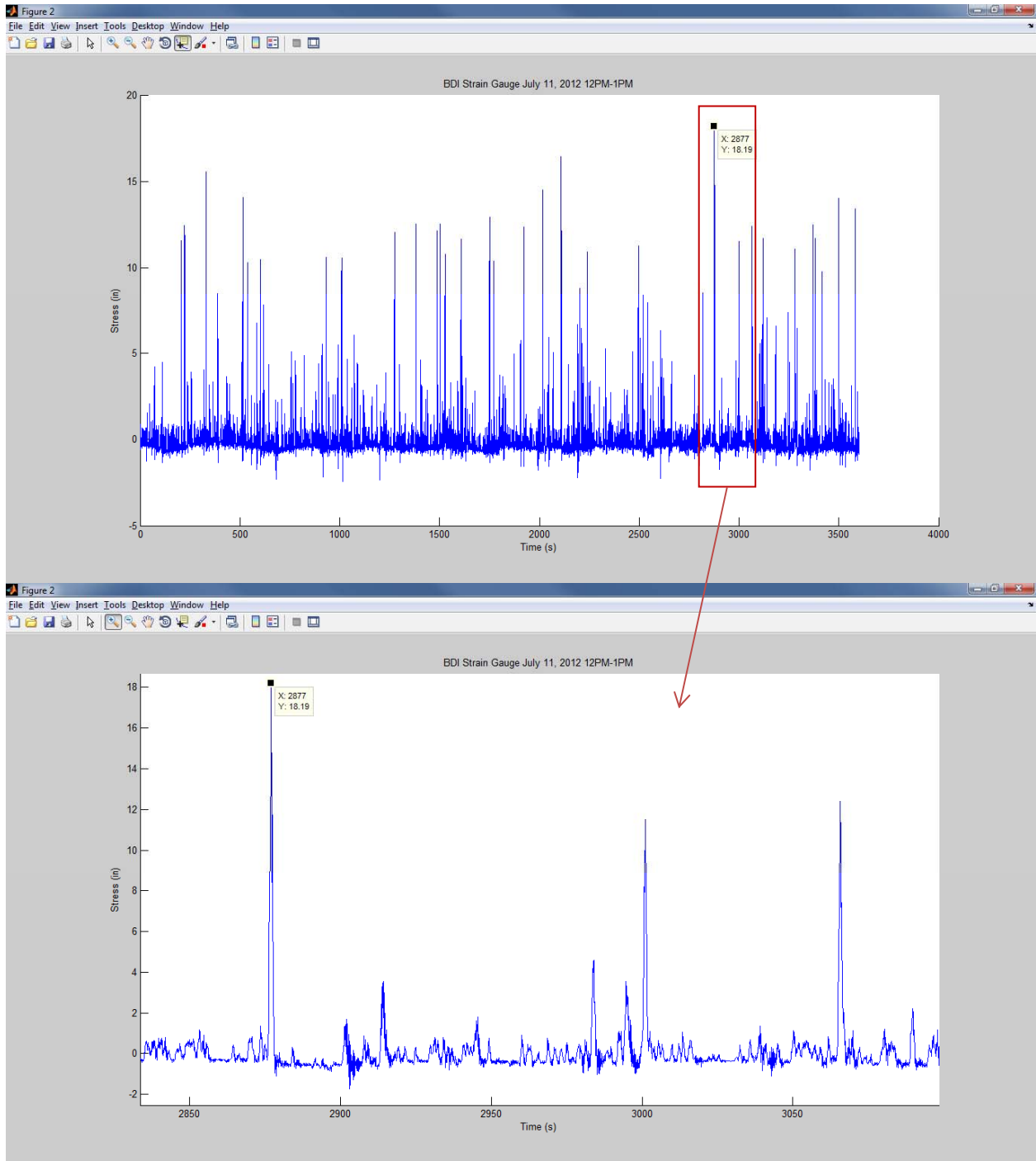
Figure 6 – Sample segment 4 of the continuously monitored strain data

By Tim Saad and Chung C. Fu

Four sets of sampled AE events (peaks) with their corresponding stresses are shown here. Data were collected remotely and these sampled results are dated 7/14/12 and 7/15/12. The first chart of the 4 chart set in the following figures portrays the time history of stress data for one-hour of data. The AE event that occurred during this time is portrayed with a green dot. The second chart provides a more detailed (zoomed-in) view of the stress data, with the AE event portrayed with a green dot at the time of its occurrence. The last chart shows the voltage data from the AE event which was previously depicted by the green dot.
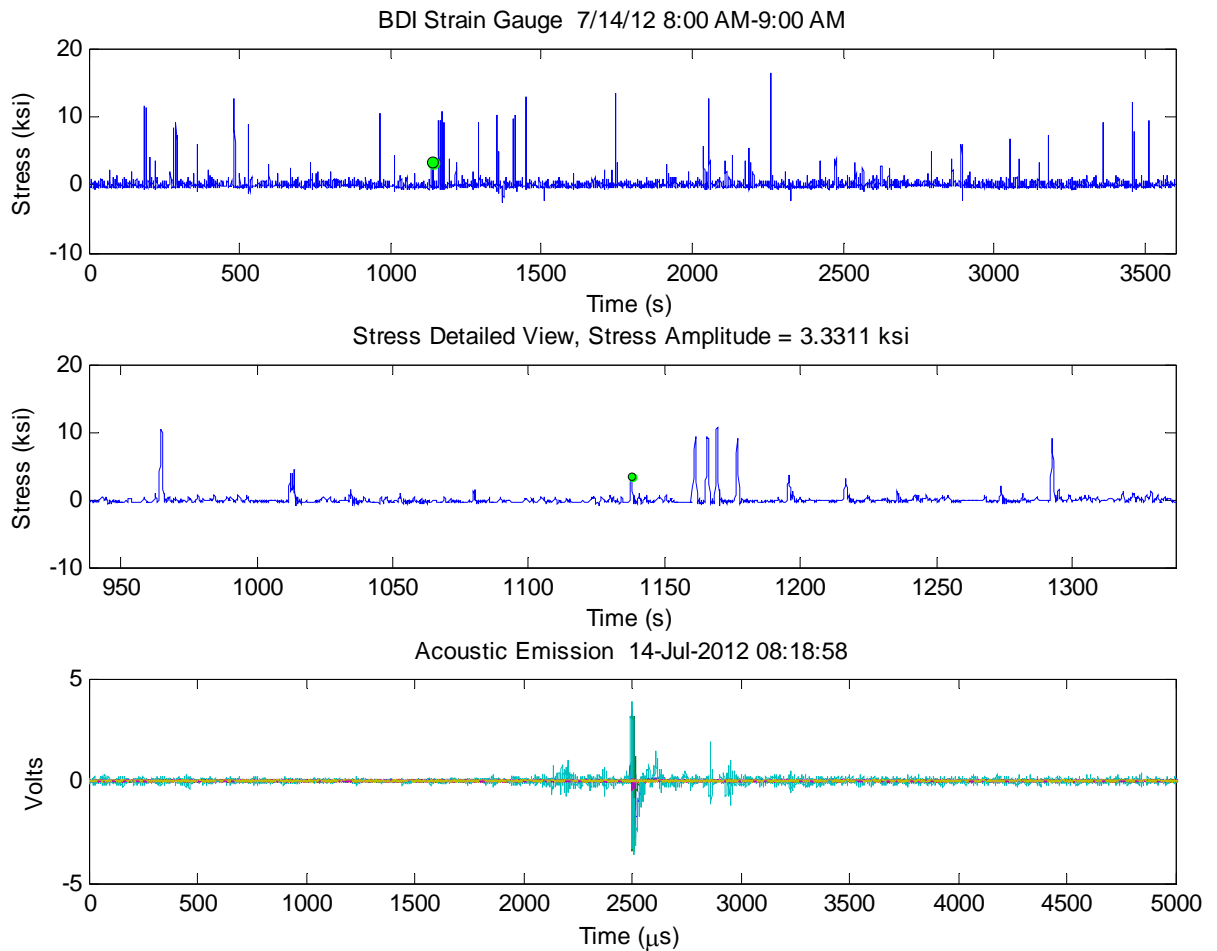
Figure 1 – Data 8-9 am 7/14/12 (a) Stress within one-hour period, (b) zoom-in data and (c) AE event
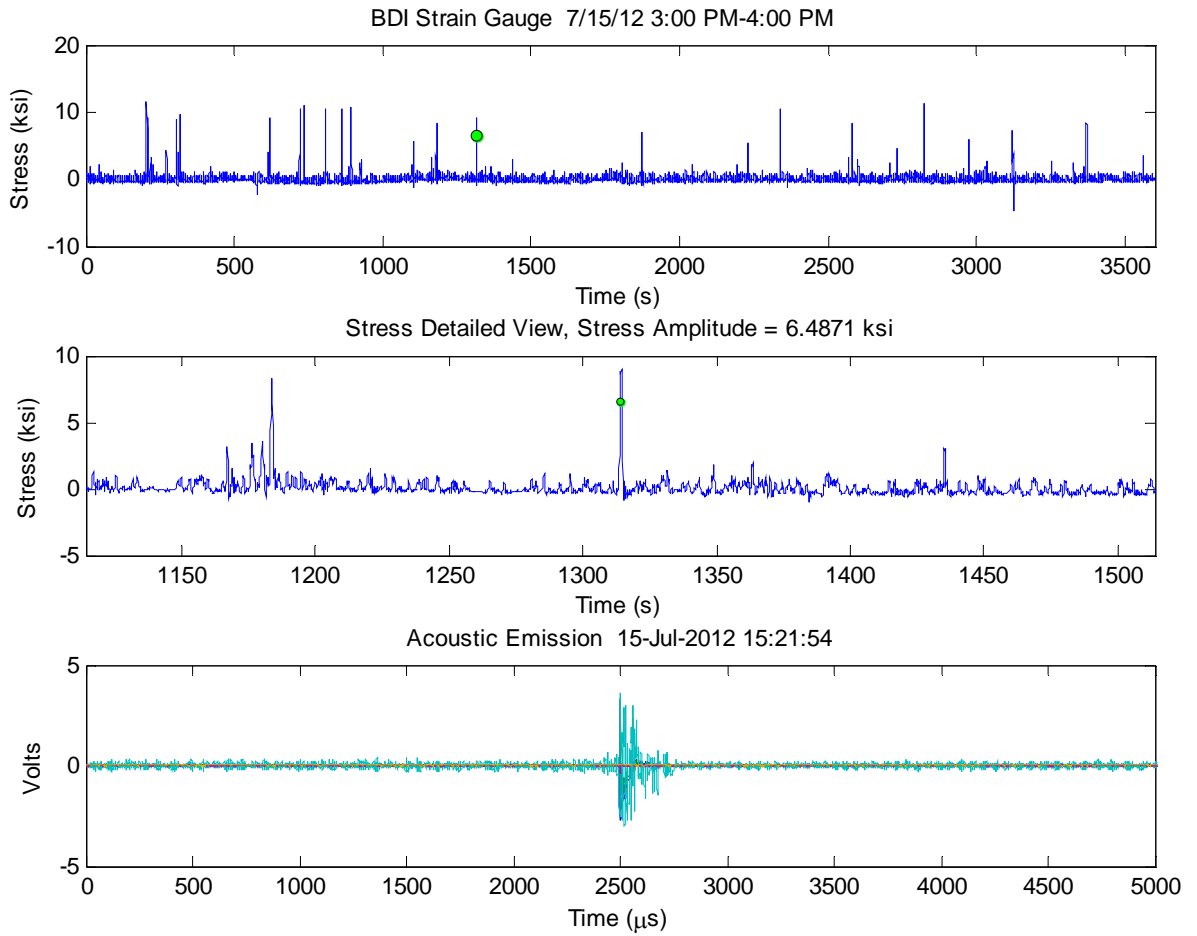
Figure 2 – Data 3-4 pm 7/15/12 (a) Stress within one-hour period, (b) zoom-in data and (c) AE event
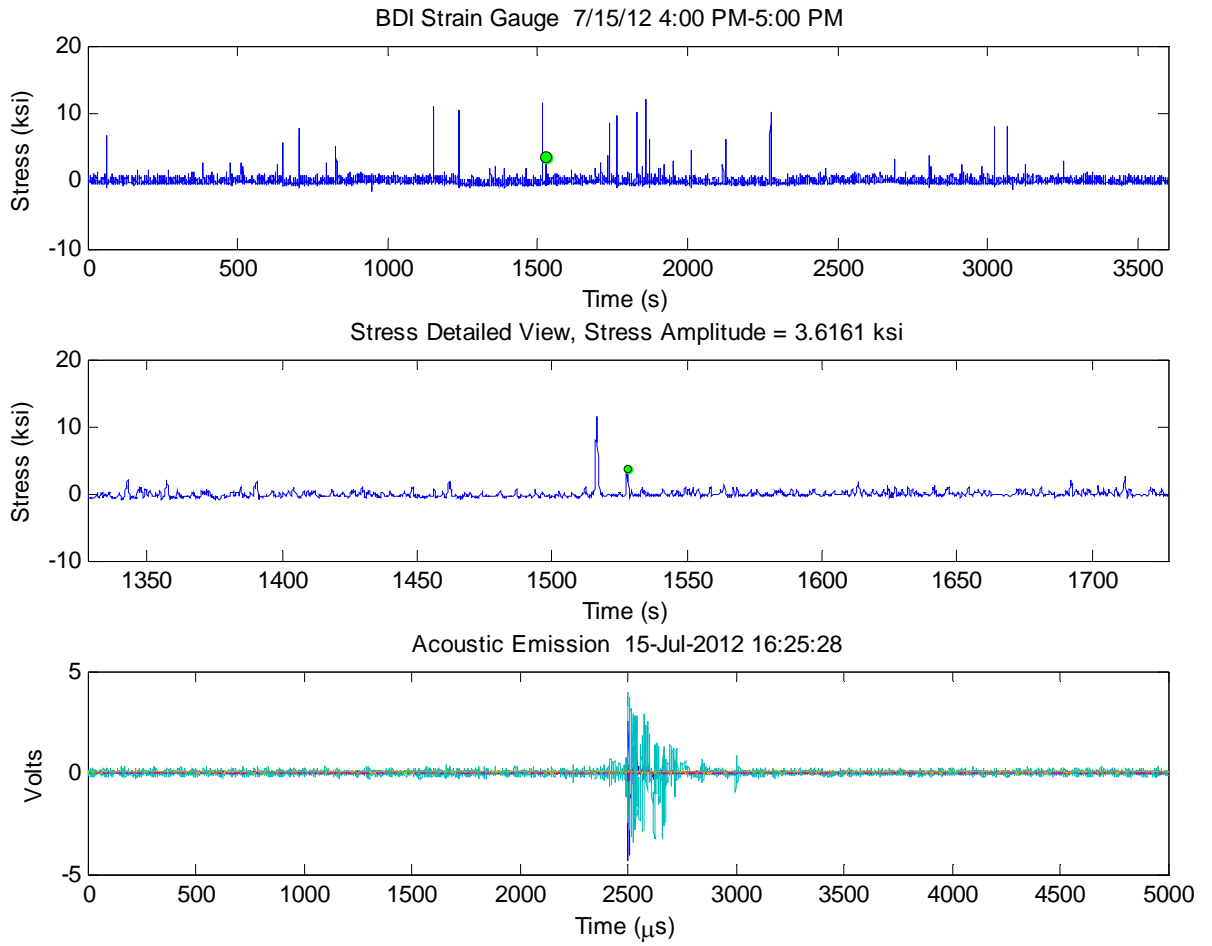
Figure 3 – Data A 4-5 am 7/15/12 (a) Stress within one-hour period, (b) zoom-in data and (c) AE event
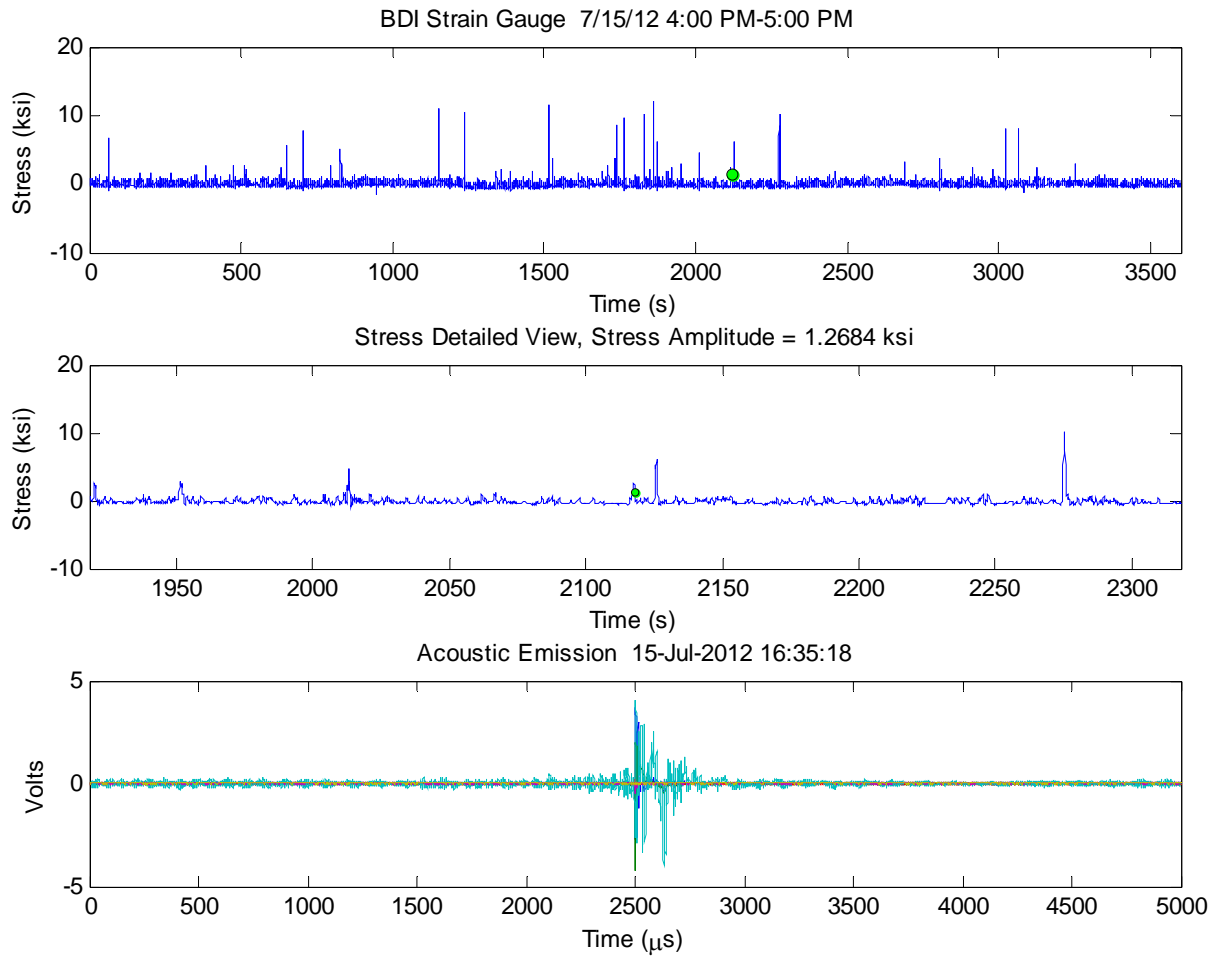
Figure 4 – Data B 4-5 pm 7/15/12 (a) Stress within one-hour period, (b) zoom-in data and

Appendix D - Traffic Loading Simulation and Bridge Finite Element Analysis

By Gengwen Zhao and Chung C. Fu

1. Traffic Data

This is a continuing study of the traffic loading simulation contained in Appendix C of the 5th progress report. The data that has been used to simulate traffic flow is the time varying vehicle count data from Internet Traffic Monitoring System operated by Maryland Department of Transportation State Highway Administration. (http://shagbhisdadt.mdot.state.md.us/ITMS_Public/default.aspx)

However, there are some problems with these vehicle count reports. The dates of these vehicle count reports are long time ago, from 2001 to 2008, mostly in spring or October. The durations of these reports are all less than 24 hours. That cannot match with our field test.

The data mostly met our need is the continuous Weigh-In-Motion data for trucks on the bridge of I270 (Southbound) over Middlebrook Road near Germantown, Maryland, probably lasting more than one week during summer and winter 2012. Since the nearby station -Hyattstown southbound station does not have what we want; we have to contact other institutions trying to get continuous traffic flow data. Further search on traffic data is still ongoing and further study will be made once the data is received.

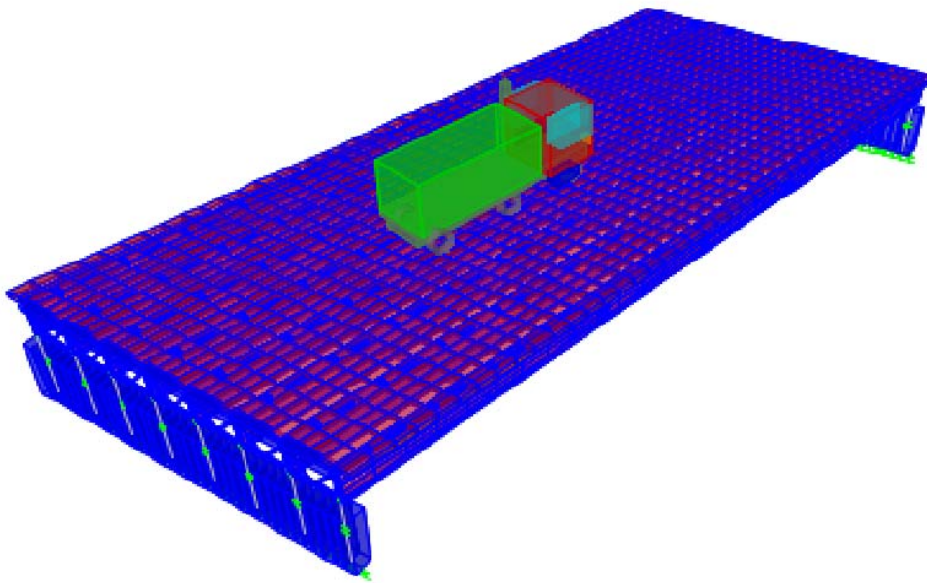Figure 1 shows the schematic view of a truck on the Middlebrook Bridge FE model.

Figure 1. Bridge under Traffic Loading

2. Finite Element Model

A.   Global Model

Once the traffic data is collected, it will be simulated to the bridge model by the CSiBridge program. This part is to refine the global and local models for the crack locations of the Maryland Middlebrook Bridge contained in Appendix C of the 5th progress report. Figure 2 shows the displacement time history of midpoints at the bottom flange for Girder 3 and Girder 4. The maximum differential displacement is 0.08 in under simulated traffic loading. Figure 3 shows the time history curves of two hot spots of the connection plate, located at Girder 3 Diaphragm 3. Shell element 252 is on the G3crack side, and shell element 250 is on G3 uncrack side. Both of them are on the same face.

Graphic results are shown below. Figure 4 shows the crack locations on Girders 3 and 4 on the bridge model. Figures 5 and 6 show zoom-in stress contours of connection plates on Girder 3 Diaphragm 3 at T=597second and on Girder 4 Diaphragm 3 at T=283second, respectively.
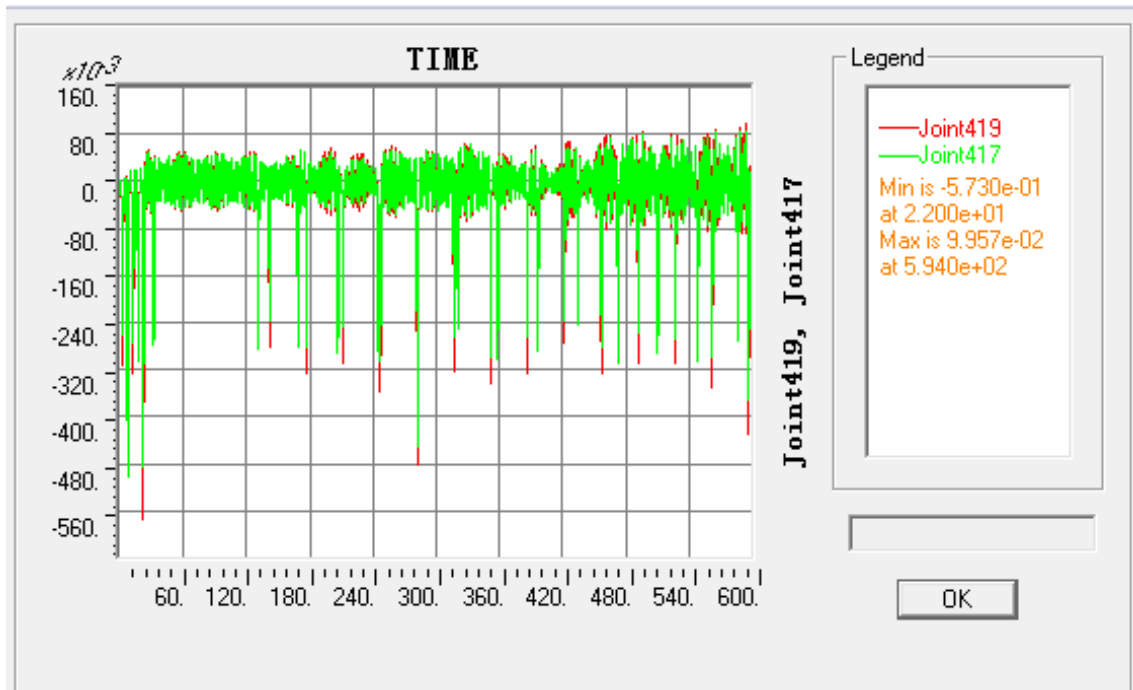
Figure 2-Midpoint displacements for G3(Joint 419) and G4(Joint417),unit - inches
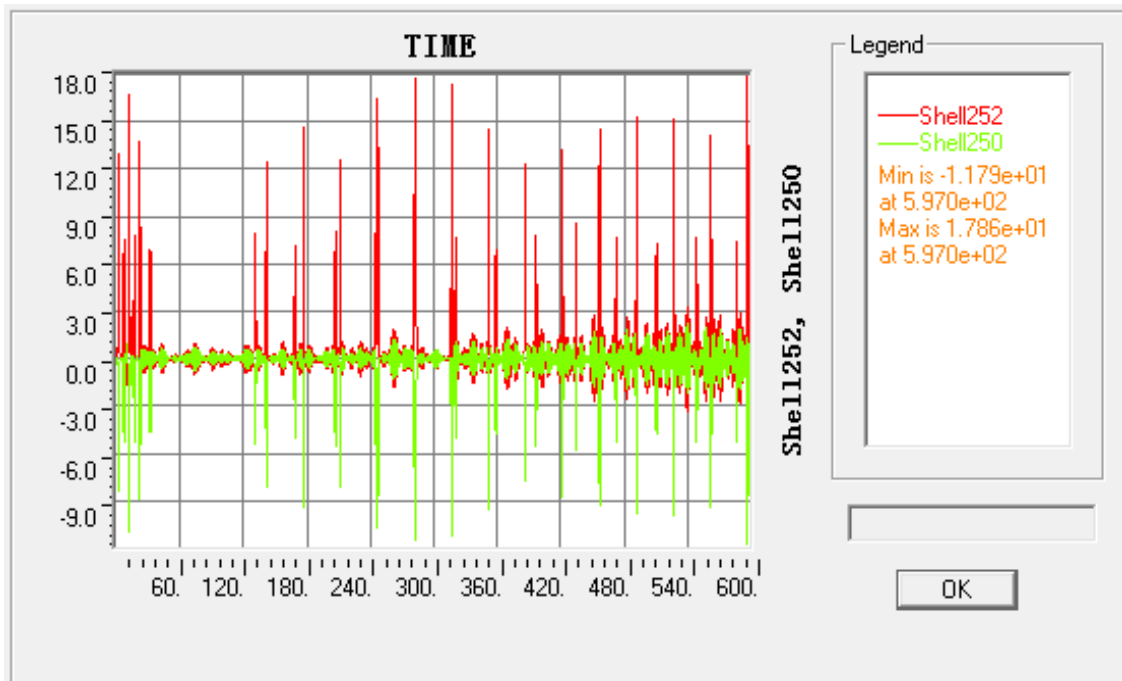
Figure 3-Stress of Hot Spot (Shell252-G3crack side, shell250-G3uncrack side)
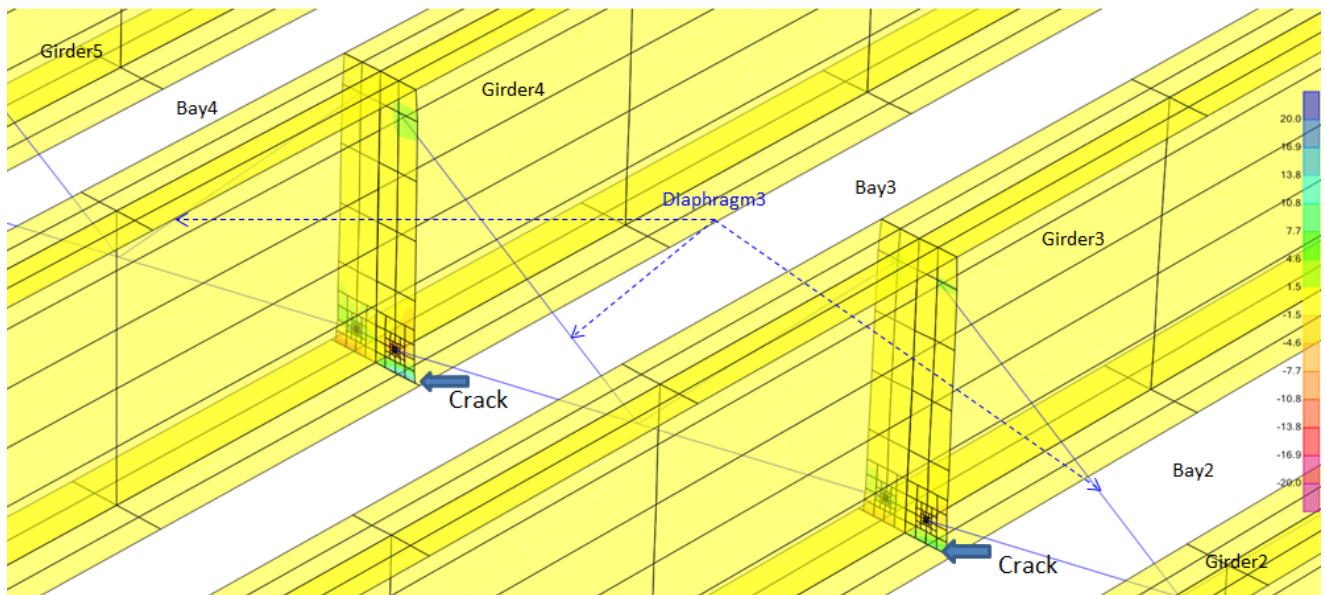unit-ksi
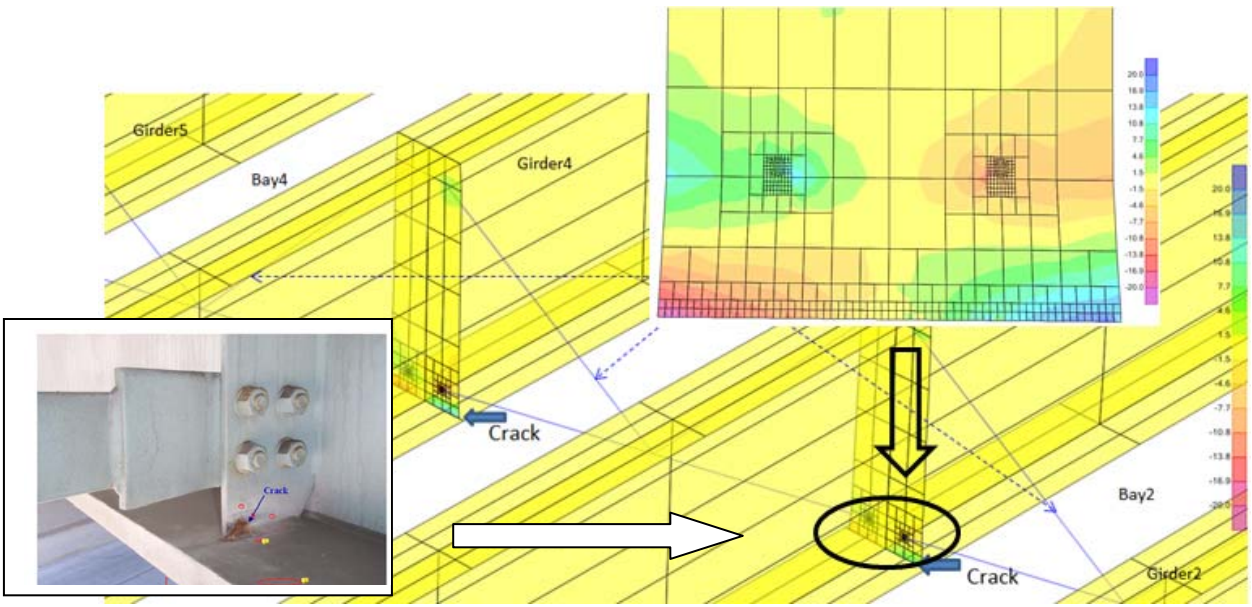

Figure 4 - Crack Locations

Figure 5 - Zoom-in Stress Contour of Connection Plate (Girder 3 Diaphragm 3) at T=597second
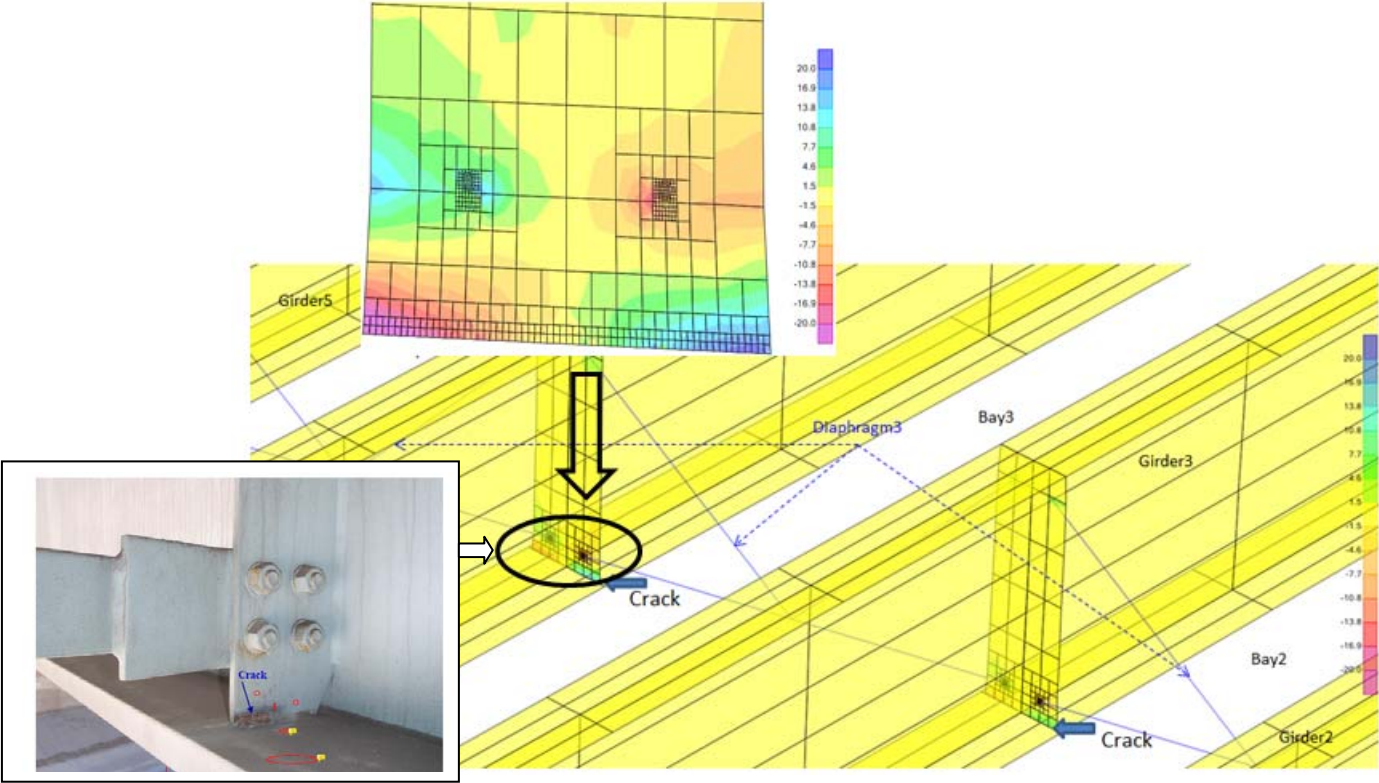

Figure 6 - Zoom-in Stress Contour of Connection Plate (Girder 4 Diaphragm 3) at T=283second

B. Local Model

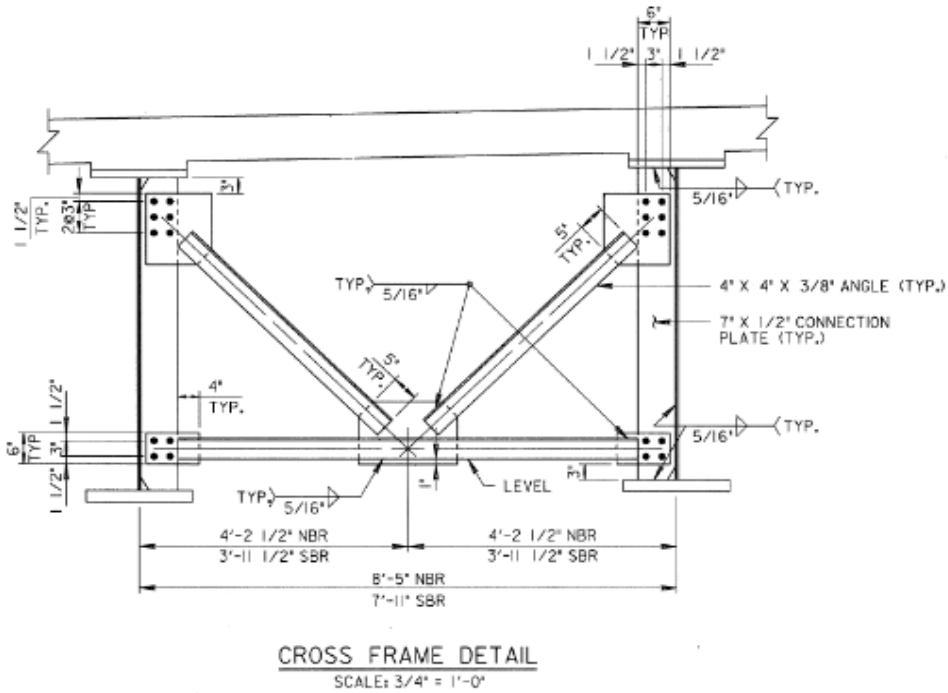Figure 9 shows the plan for typical K-type cross frame detail and Figure 10 shows the finite element local model in SAP 2000.
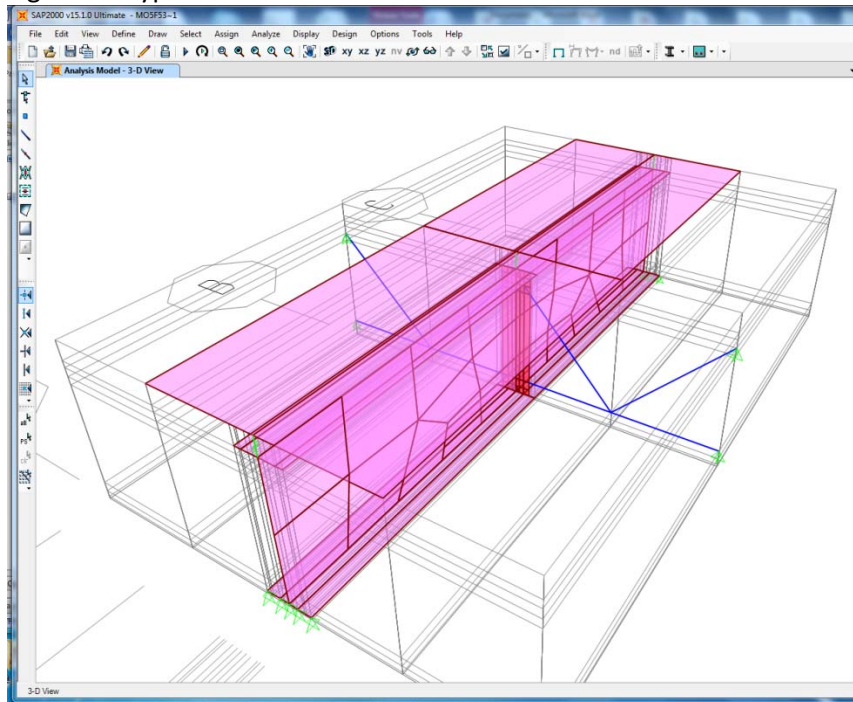

Figure 9 - Typical cross frame detail

Figure 10 - Local model at mid span girder three

The model and its results are summarized below:

1) Local Model – portion of girder with K-type crossframes on both sides (Figure 10)
2) Boundary condition - pin supported (Figure 10)
3) Loading - 0.2in downward displacement on the left end and 0.4in upward displacement at the right end were applied (Figure 10)
4) Maximum stress around bottom chord and connection plate connection (Figure 11)
   -1.7ksi compressive stress on the left connection plate
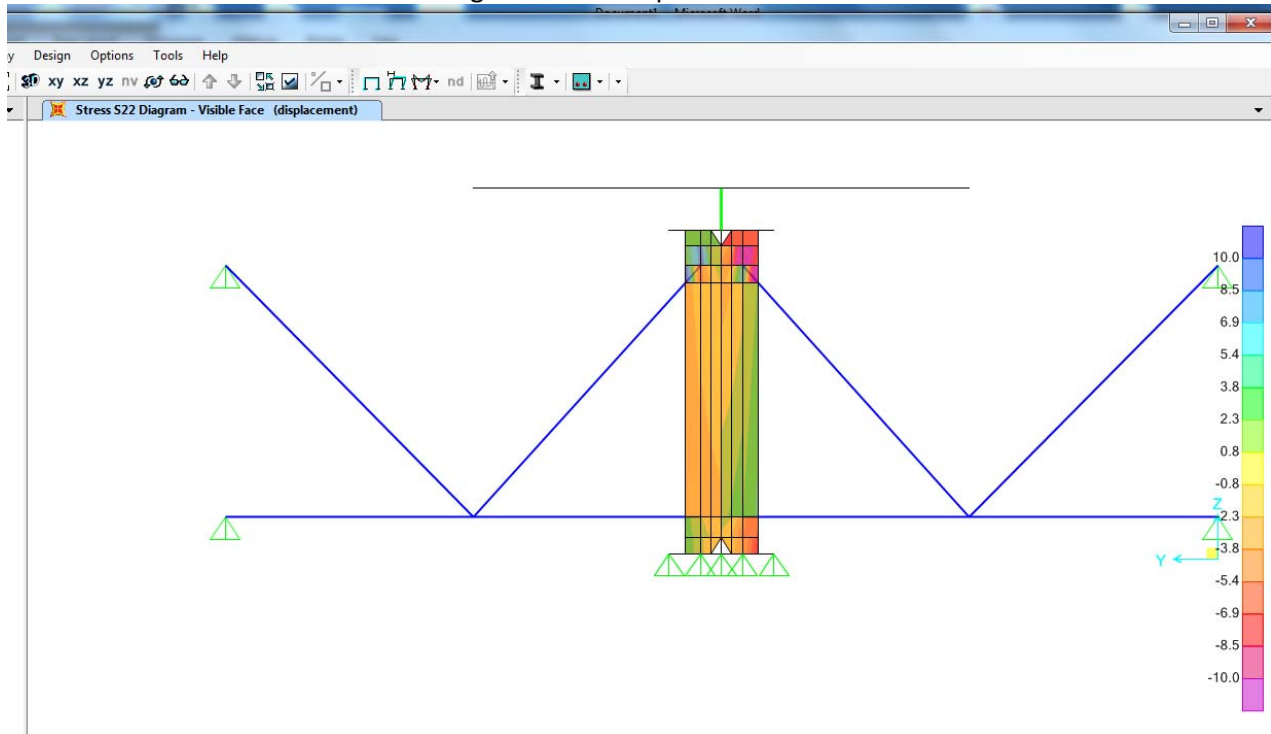   +4.07ksi tensile stress on the right connection plate

Figure 11 - Local model stress contour on connection plate

It can be concluded that among all types of cross-frames, X-type with top and bottom chords is the stiffest of all, then the K-type with top and bottom chords, then the X-type with bottom only and the flexible one is the K-type with bottom chord only. Differential displacement between girders will cause one diagonal in tension and one in compression. Since the working point of the diagonal is not at the junction of girder web and top flange plus no help from the top chord, one side of the connection plate will be under tension and one under compression. Measured 16.1 ksi in tension is not surprising with the flexibility of the cross-frame and the girder system (with up to 0.5" to 0.75" vertical deflections due to live load observed.)

Appendix E - Test Plan for Field Test on I-270/Middlebrook Bridge

Date: May 29 and 30, 2013, 9:00am to late afternoon
Bridge Site: latitude=39.175296, longitude= -77.247046, I-270 exit at middlebrook road (near Germantown).

- *Sensor degradation in the field environment:*
1. Guard paint sensor connection problem. The guard sensor was put on in the field tests last November 14 and 15. After exposed in the wild for the whole winter, the connection was peeled off due to lack of protection. This can be clearly seen in Figure 1.

Figure 1. Guard sensor connection peeled off.

2. Sensor affected by humidity.

For the sensors near the fatigue crack, they were covered by plastic film as shown in Figure 2. After the whole winter, the connections between the wire and the sensor were still good. However, some sensors have short circuit between the sensor output and the ground, which results in the failure discussed before. A sample case of short circuit is shown in Figure 3 as shown by the multimeter. However, the paint sensor in the lower left was still good. According to this examination, it is confirmed that the plastic film protects the sensor from humidity at some degree.

Figure 2. AE sensors near fatigue crack were covered by plastic film to protect from humidity.

Figure 3. Short circuit of AE sensors near fatigue crack due to the humidity.

- *Sensor replacement and wireless sensing incorporation*

3. Sensor replacement

All the sensors are replaced including the guard sensor in this test. The newly replaced sensors are illustrated in Figure 4. Sensor a0 and a1 are AE sensors made of PZT5A and both have the same diameter-5mm. For sensor a2 and a3, they are made of piezo paint and they have a ½" diameter. Their relative positions are shown in Figure 5. In order to further protect the sensors from humidity, a layer of polyurethane coating was applied on the sensors for extra protection besides the plastic film protection as shown in Figure 6.
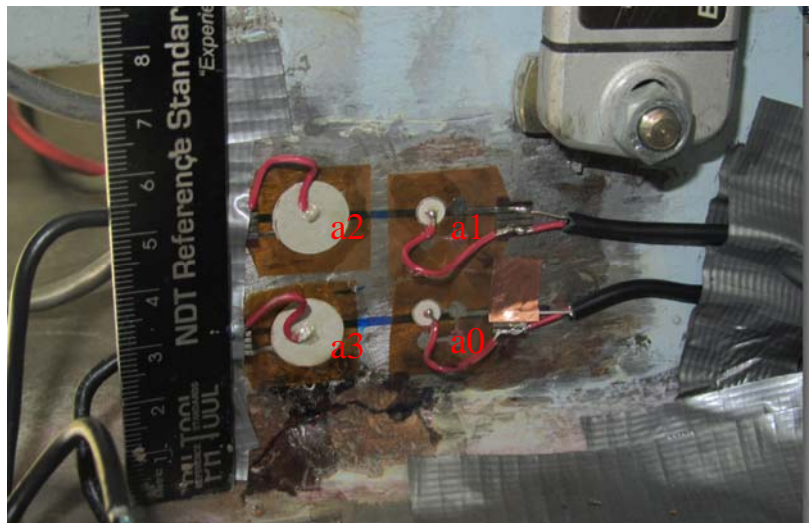
Figure 4. Newly installed sensor near the fatigue crack (a layer of polyurethane coating was applied on the sensors for extra protection of humidity).
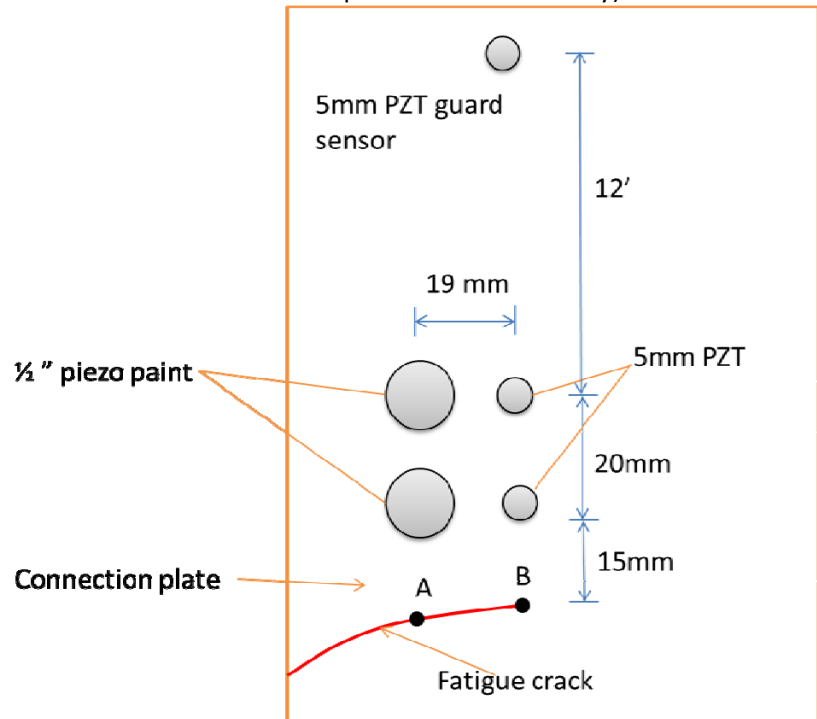

Figure 5. Schematics of sensor locations

(a)   (b)

Figure 6. Newly installed sensor covered by plastic film: (a) guard sensor; (b) sensors near the fatigue crack.

4. Pencil lead break test data

As a standard simulated AE source, pencil lead break tests were carried for calibration purpose. The test set up is shown in Figure 7. Figure 8 shows the signals and their frequency spectra due to a pencil lead break event captured by all the five sensors including the guard sensor. It can be seen that the guard sensor has nearly no response since it's far away from the simulated source.
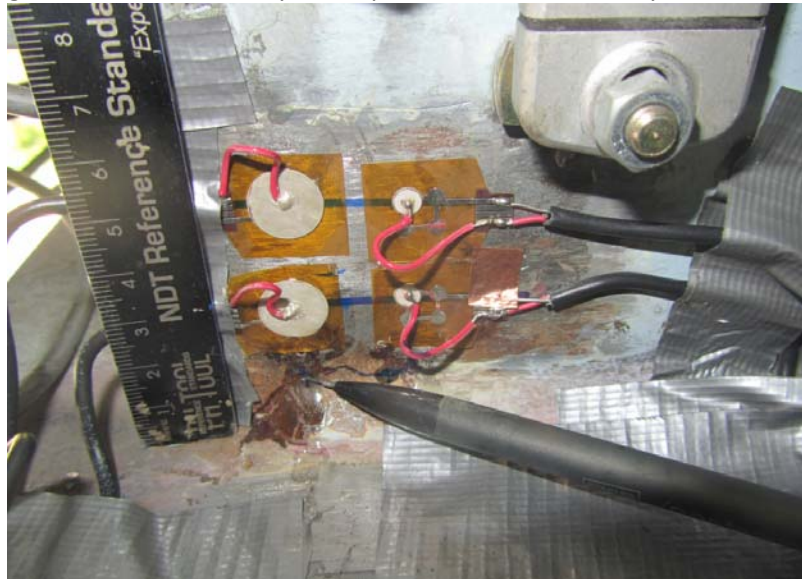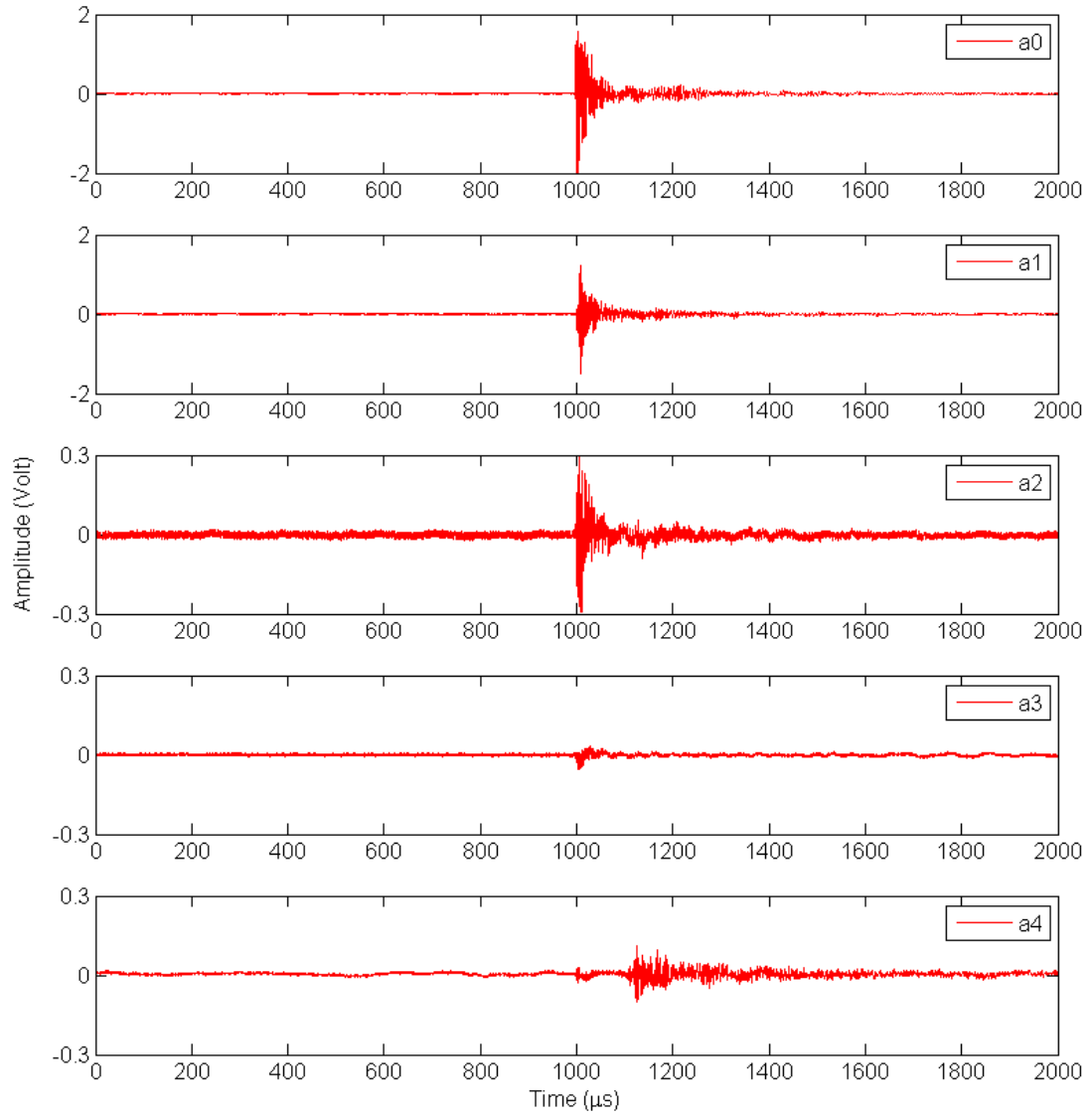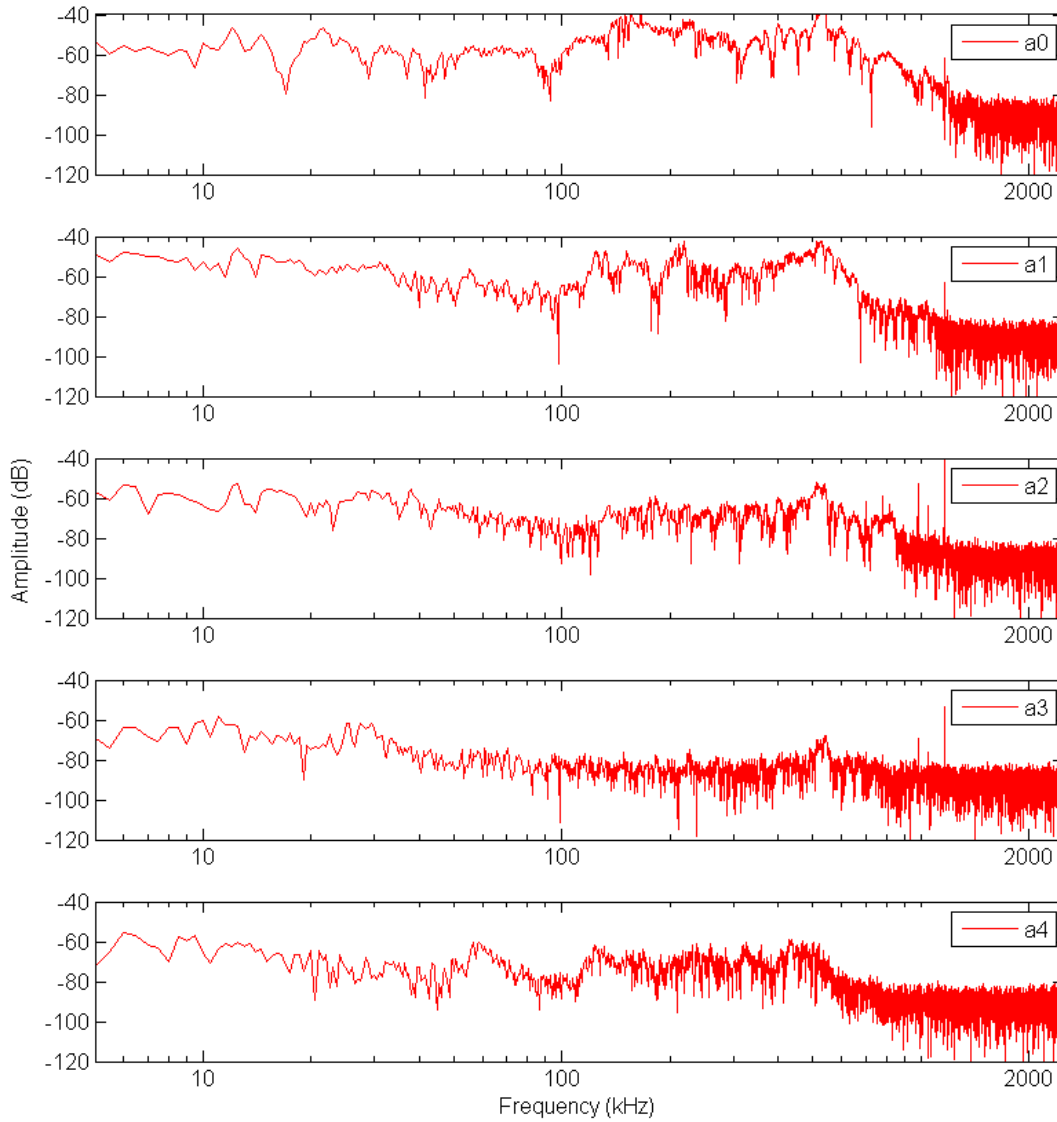

Figure 7. Pencil lead break test at the middle point of the fatigue crack.

(a)

(b)

Figure 8. Sensor signals due to pencil lead break test at the middle point of the fatigue crack: (a) signal waveform; (b) frequency spectrum

5.   Integration with wireless sensor from NCSU

Channel 0 was connected to wireless sensor. Pencil lead break tests were carried out and traffic induced signals were captured. Figure 9 shows the system set up for the wireless sensor near the fatigue crack and Figure 10 shows the status of wireless sensor storing captured signal. Figure 11 shows the base station for receiving signals at the abutment. This base station was connected to PXI through USB.

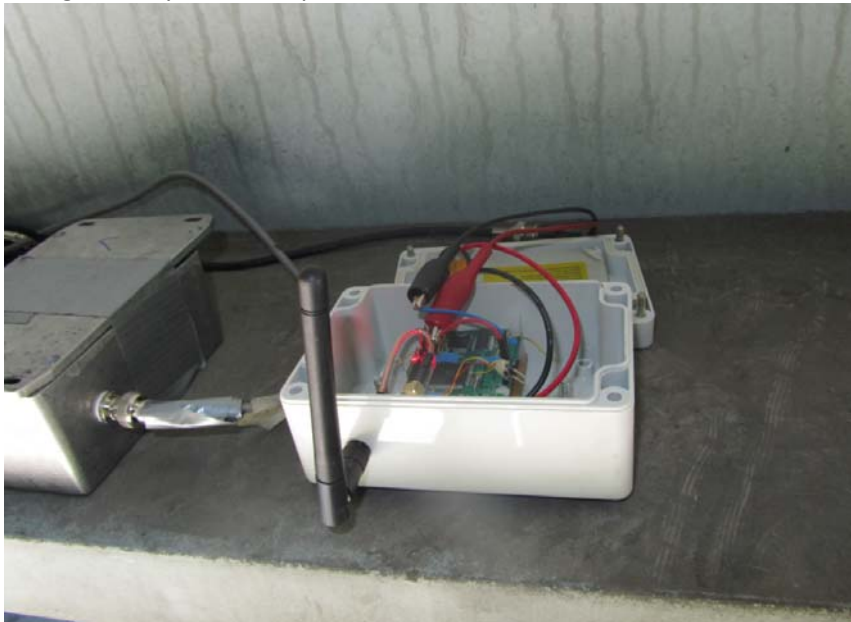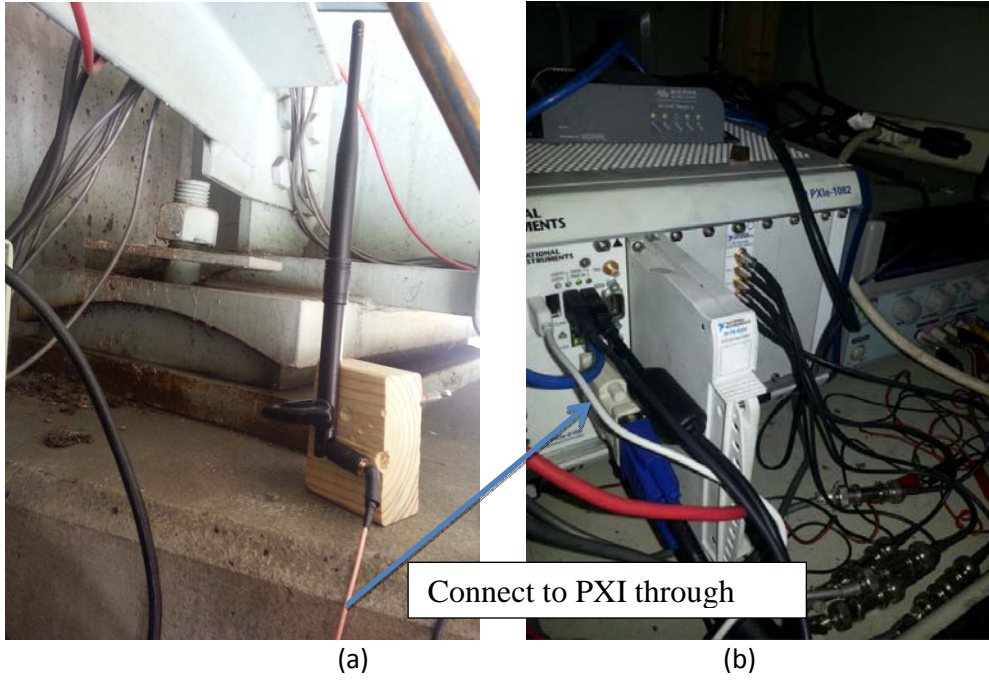Figure 9. System set up overview with the wireless sensor

Figure 10. Wireless sensor was triggered.

Connect to PXI through

(a)   (b)

Figure 11. Wireless sensor receiver at the abutment:
(a) base station (b) connection to PXI with USB.